

2012-10-03

Wellbore Strengthening- Nano-Particle Drilling Fluid Experimental Design Using Hydraulic Fracture Apparatus

Nwaoji, Charles Okeibuno

Nwaoji, C. O. (2012). Wellbore Strengthening- Nano-Particle Drilling Fluid Experimental Design Using Hydraulic Fracture Apparatus (Master's thesis, University of Calgary, Calgary, Canada).

Retrieved from <https://prism.ucalgary.ca>. doi:10.11575/PRISM/28685

<http://hdl.handle.net/11023/279>

Downloaded from PRISM Repository, University of Calgary

UNIVERSITY OF CALGARY

Wellbore Strengthening- Nano-Particle Drilling Fluid Experimental Design Using Hydraulic
Fracture Apparatus

by

Charles Okeibuno Nwaoji

A THESIS

SUBMITTED TO THE FACULTY OF GRADUATE STUDIES
IN PARTIAL FULFILMENT OF THE REQUIREMENTS FOR THE
DEGREE OF MASTER OF SCIENCE

DEPARTMENT OF CHEMICAL AND PETROLEUM ENGINEERING
CALGARY, ALBERTA

SEPTEMBER, 2012

© Charles Okeibuno Nwaoji 2012

Abstract

This research project introduces novel lost circulation material (LCM) drilling fluid blends for both water based mud (WBM) and invert emulsion (diesel oil) based mud (OBM) that have been used successfully in the laboratory to achieve very impressive wellbore strengthening results in both permeable and impermeable formations. The optimal blends consisting of in-house prepared nanoparticles (NP1 and NP2) and standard LCM-graphite were established by running and analyzing laboratory hydraulic fracture tests on Roubidoux sandstone and concrete cores.

Different blends were used to induce and seal fractures in the cores. The blends that increased the core fracture breakdown pressure (fbp) the most with minimal distortion in mud rheological properties were selected as optimal blends.

The optimal WBM blend increased the core fbp by 70.31% while the optimal OBM blend increased the core fbp by 36.39%. Impermeable concrete tests indicate a positive application of the tested blends in shale formation wellbore strengthening.

Acknowledgements

I would like to specially thank my supervisor Dr. Geir Hareland for giving me the opportunity to work on this project and for believing in me. My sincere appreciation also goes to my co-supervisor Dr. Maen Husein and my project advisor Dr. Runar Nygaard from Missouri University of Science and Technology. I want to thank you all for the invaluable technical and motivational support rendered throughout the course of this work.

My thanks also go to Mr. Maximiliano Liberman, Mr. Steven Hilgedick and Mr. Sudarshan Govindarajan for all their assistance and support in running the hydraulic fracture experiments.

Many thanks to Mrs. Patricia Teichrob and everyone in the Drilling Engineering Research Group at the University of Calgary for all their support during the course of my graduate studies.

I would also like to express my profound gratitude and appreciation to the following organisations: NSERC, Talisman Energy Inc. and Pason Systems for funding this research work.

Dedication

I would like to dedicate this work to my mum, my wife and lovely kids, for putting up with my long sojourn away from home and for all their prayers and emotional support.

Table of Contents

| | |
|--|--------|
| Abstract | ii |
| Acknowledgements | iii |
| Dedication | iv |
| Table of Contents | v |
| List of Tables | vii |
| List of Figures and Illustrations | viii |
| List of Symbols, Abbreviations and Nomenclature | x |
| Epigraph | xi |
| CHAPTER ONE: INTRODUCTION | 1 |
| 1.1 Lost circulation while drilling | 1 |
| 1.1.1 Narrow mud weight window | 3 |
| 1.1.2 Fracture breakdown pressure prediction | 5 |
| 1.2 Literature review | 5 |
| 1.2.1 DEA 13 experiments | 6 |
| 1.2.2 GPRI experiments | 8 |
| 1.2.3 Wellbore strengthening mechanisms | 9 |
| 1.2.3.1 Stress cage | 9 |
| 1.2.3.2 Fracture closure stress | 10 |
| 1.2.4 Nano-particles | 12 |
| 1.3 Research objectives | 14 |
| CHAPTER TWO: EXPERIMENTAL DESIGN PARAMETERS AND HYDRAULIC FRACTURE APPARATUS SET-UP | 17 |
| 2.1 Experimental parameters | 17 |
| 2.1.1 Uncontrollable parameter | 17 |
| 2.1.2 Fixed parameters | 17 |
| 2.1.3 Variable parameters | 18 |
| 2.2 Hydraulic fracture apparatus set up | 18 |
| 2.2.1 Pump system and fluid distribution | 21 |
| 2.2.2 Accumulator | 22 |
| 2.2.3 Hydraulic piston | 23 |
| 2.2.4 In-line pressure regulator | 23 |
| 2.2.5 Rubber sleeve | 24 |
| 2.2.6 Stainless steel cylinder | 24 |
| 2.2.7 All thread rods | 24 |
| 2.2.8 Bottom flange | 24 |
| 2.2.9 Top flange | 25 |
| 2.2.10 Hydraulic fracture apparatus frame | 25 |
| 2.2.11 Data acquisition | 25 |
| CHAPTER THREE: EXPERIMENTAL PROCEDURES FOR HYDRAULIC FRACTURE OPERATION | 26 |
| 3.1 Core sample preparation procedure | 26 |
| 3.1.1 Drilling out cylindrical cores | 27 |

| | |
|---|----|
| 3.1.2 Cutting core surface with slab saw | 27 |
| 3.1.3 Grinding core using a surface grinder | 28 |
| 3.1.4 Drilling borehole in core | 29 |
| 3.1.5 Fixing steel caps to core | 29 |
| 3.1.6 Vacuuming core..... | 30 |
| 3.1.7 Soaking core in water | 30 |
| 3.1.8 Concrete core preparation..... | 30 |
| 3.2 Hydraulic fracture apparatus operation procedure..... | 31 |
| 3.3 Fracturing fluid mixing procedure..... | 32 |
| 3.4 Rock tensile stress measurement procedure | 35 |
| CHAPTER FOUR: RESULTS AND DISCUSSION | 37 |
| 4.1 Water based mud (WBM) data analysis | 38 |
| 4.2 Oil (Diesel) based invert emulsion mud (OBM) data analysis | 47 |
| 4.3 Observed differences in fracture breakdown pressures (fbp) between invert emulsion (diesel oil) based mud (OBM) and water based mud (WBM)..... | 50 |
| 4.4 Concrete test data analysis (Impermeable formation test)..... | 52 |
| 4.5 Experimental observations showing the absolute sealing effect of fracturing fluid | 55 |
| 4.6 Why Nano-particles (NPs) react better with WBM than with OBM..... | 58 |
| 4.7 Lessons learned..... | 59 |
| 4.7.1 Core sample preparation operations | 59 |
| 4.7.2 Hydraulic fracture operations | 60 |
| CHAPTER FIVE: CONCLUSIONS | 61 |
| CHAPTER SIX: RECOMMENDATIONS | 63 |
| REFERENCES | 65 |
| APPENDIX A: PRESSURE CELL ASSEMBLY AND EXPERIMENTAL SET UP CHECK LIST | 67 |
| APPENDIX B: CORE PREPARATION PICTURES | 72 |
| APPENDIX C: ROCK TENSILE STRENGTH MEASUREMENT PICTURES | 81 |

List of Tables

| | |
|--|----|
| Table 3.1: Showing the concentration percentage level set for both Nano-particles (NPs) and Granular particles | 33 |
| Table 3.2 : Showing the fracture fluid mixture recipe for water based mud | 34 |
| Table 3.3: Showing the ingredient composition and cocn of the OBM..... | 35 |
| Table 3.4: Core rock properties | 36 |
| Table 4.1: Showing the blend type and set concentration (cocn) level | 38 |
| Table 4.2: Showing fbp and the % increase of fbp of blended DFs over unblended DF for WBM..... | 40 |
| Table 4.3: Mud density and rheological properties of various WBM blends | 43 |
| Table 4.4: Showing fbp and % increase of fbp of blended inverts over unblended invert DF..... | 48 |
| Table 4.5: Showing rheological properties of invert (diesel oil) based DF blends..... | 48 |
| Table 4.6: Showing significant differences in OBM and WBM control samples fbp | 51 |
| Table 4.7: Showing the fbp of different blends and the % increase in fbp achieved in concrete cores | 53 |

List of Figures and Illustrations

| | |
|---|----|
| Figure 1.1: Illustrations showing lost circulation zones | 2 |
| Figure 1.2: Typical narrow mud weight window..... | 4 |
| Figure 1.3: Fracture growth in water based and oil based mud | 8 |
| Figure 1.4: Fracture propagation saw tooth characteristics in water based mud | 8 |
| Figure 1.5: Stress caging mechanism..... | 10 |
| Figure 1.6: Fracture closure stress (FCS) mechanism | 12 |
| Figure 1.7: Showing aggregate of nano-particles plugging a pore throat..... | 13 |
| Figure 1.8: A particle size scale | 14 |
| Figure 1.9: Surface area to volume ratio of same volume of materials | 14 |
| Figure 2.1: Schematic of hydraulic fracture apparatus system | 19 |
| Figure 2.2: Hydraulic fracture apparatus | 20 |
| Figure 2.3: Isco DX100 syringe type pumps | 21 |
| Figure 2.4: Mud accumulator system..... | 22 |
| Figure 2.5: Overburden piston | 23 |
| Figure 2.6: Bleed-off valve | 24 |
| Figure 4.1: Plot showing original breakdown pressure and re-opening pressure of core using control sample for WBM | 39 |
| Figure 4.2: Plot showing fracture breakdown pressures (fbp) for various WBM blends | 40 |
| Figure 4.3: Showing optimal blends of NP1 and NP2 in combination with graphite and the same optimal blends in combination with calcium carbonate | 42 |
| Figure 4.4: A typical NP1 blend in a mud mixer..... | 45 |
| Figure 4.5: A typical NP2 blend in a mud mixer..... | 45 |
| Figure 4.6: Fractured sandstone core showing both vertical and horizontal fractures | 46 |
| Figure 4.7: Cross section of fractured core showing the leak off effect | 46 |

| | |
|--|----|
| Figure 4.8: Plot showing fbp for invert emulsion (diesel oil) mud using established optimal blends 3 and 8 | 47 |
| Figure 4.9: Typical OBM blend..... | 49 |
| Figure 4.10: Vertically fractured sandstone core using OBM blend | 49 |
| Figure 4.11: Showing differences in fbp between WBM and OBM control samples | 51 |
| Figure 4.12: Showing the fbp of optimal WBM blends and fbp of the same blends in OBM | 52 |
| Figure 4.13: Showing fbp of different blends using concrete cores | 53 |
| Figure 4.14: Induced vertical fracture in concrete core | 54 |
| Figure 4.15: Two vertically induced fractures using blend 4 on sandstone core..... | 56 |
| Figure 4.16: Showing re-opening pressure fbp as high as original fbp for the blend 4 test | 56 |
| Figure 4.17: Two vertically induced fractures using blend 8 on concrete core | 57 |
| Figure 4.18: Showing re-opening pressure fbp as high as original fbp for the blend 8 test | 57 |

List of Symbols, Abbreviations and Nomenclature

| Symbol | Definition |
|--------------|--|
| A | Granular particle (graphite) |
| B | Granular particle (calcium carbonate) |
| DEA | Drilling Engineering Association |
| DF | Drilling fluid |
| ECD | Equivalent circulating density (ppg) |
| fbp | Fracture breakdown pressure |
| FCS | Fracture closure stress (psi) |
| LCM | Lost circulation material |
| LOT | Leak off test |
| NPs | Nano-particles |
| NP1 | Iron (III) hydroxide nano-particles |
| NP2 | Calcium carbonate nano-particles |
| OBM | Invert emulsion (diesel oil) based mud |
| ppg | Pounds mass per gallon |
| WBM | Water based mud |
| T_0 | Rock tensile strength (psi) |
| P_{fb} | Fracture breakdown pressure (psi) |
| P_0 | Pore pressure (psi) |
| <i>Greek</i> | |
| α | Biot's constant |
| η | Poroelastic constant |
| ν | Poisson's ratio |
| σ_h | Minimum horizontal stress (psi) |
| σ_H | Maximum horizontal stress (psi) |

Epigraph

To the extent that your work takes into account the needs of the world, it will be meaningful; to the extent that through it you express your unique talents, it will be joyful.

-Laurence G. Boldt, How to find the work you love

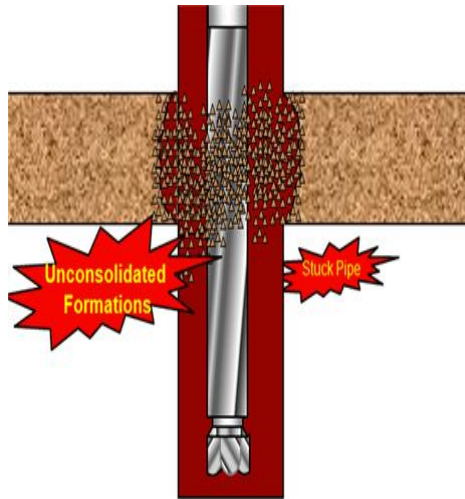
Chapter One: INTRODUCTION

1.1 Lost circulation while drilling

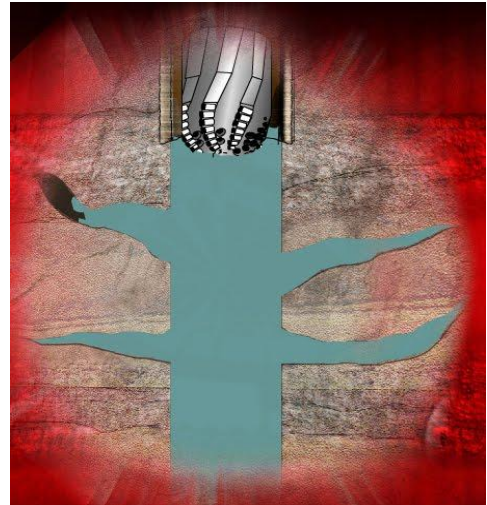
One of the frequently encountered problems and the leading cause of non productive time in drilling operations is lost circulation¹. It approximately costs the drilling industry over one billion dollars annually², resulting in wide spread interests for solutions to this very costly problem. Lost circulation is simply the loss of part or all mud to the formation at any depth while drilling. Lost circulation occurs in the following formations; permeable unconsolidated e.g. sand, shell beds, pea gravel and reef deposits; vugular and cavernous e.g. limestone, chalk, dolomite and reefs; naturally or induced fractured. Instant mud loss called natural loss circulation occurs when drilling through formations with large pores, vugs, leaky fault or natural fractures while induced mud loss circulation occurs when the imposed wellbore pressure is greater than the pressure the wellbore can contain. Induced mud loss circulation amounts to over 90% of the operator's loss returns expense³ and hence, will be the focus of this project work.

Adding to the problem of lost circulation is the loss of hydrostatic wellbore pressure resulting from mud losses, which can lead to underground or surface blow out due to the influx of formation fluid or formation collapse. Formation collapse can lead to loss of tool assemblies, blowouts and pipe sticking. These issues make it almost impossible to assess reserves in depleted zones and deep water drilling where the drilling window between pore pressure and fracture gradient is very narrow. The engineering options available to be able to drill through these zones are; drilling underbalanced, casing and cementing troublesome zones, running additional casings strings through weak zones, using expandable casing/liner, heating drilling mud to increase the hoop stress around the wellbore and wellbore strengthening. The most applicable, effective and cheapest of these methods is wellbore strengthening. The industry has been using wellbore

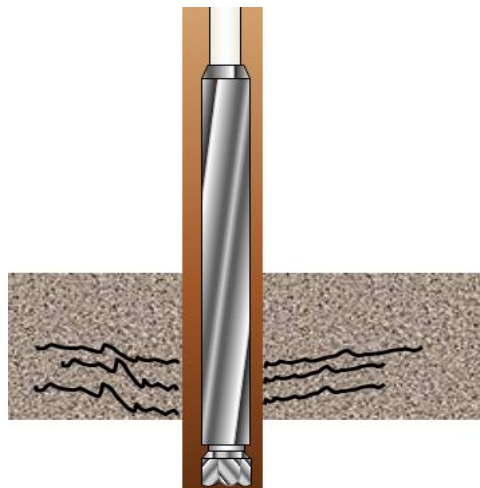
strengthening which involves combining lost circulation materials with drilling fluid, for years as preventative measures (pre-treatment of mud) or for remediation when losses occur to treat loss circulation issues. Figure 1.1 illustrates the different lost circulation zones



Unconsolidated zone



Vugular/Cavernous zone



Naturally/induced fracture zone

Figure 1.1: Illustrations showing lost circulation zones

1.1.1 Narrow mud weight window

While drilling, the mud weight pressure is usually kept between the pore pressure and fracture pressure of the formation being drilled. The mud weight window is simply the difference between the lower bound pore pressure and the upper bound fracture gradient/pressure of the formation. Wellbore pressure during drilling is maintained by the drilling fluid. When the wellbore pressure is less than the formation pressure in a permeable formation, formation hydrocarbon fluid flows into the wellbore causing a situation known as a kick. A blow out occurs as a result of formation hydrocarbon fluid influx, if the wellbore pressure is not increased and made higher than the formation pressure. To avoid this, the drilling mud pressure in the wellbore which defines the lower limit of the mud window, must be more than the borehole collapse pressure and formation pore pressure. The upper limit of the mud window is the fracture gradient. This is the pressure at which wellbore fluid will fracture the formation leading to mud loss into the formation and is determined by a leak off test (LOT) while drilling. The induced lost circulation can occur while drilling, during completion and also during cementing of the well. Thus the operating window defined by the upper bound-fracture gradient and the lower bound-pore pressure define the safe mud weight window. The wider this window, the easier it is to drill through the formation. But when this window is narrow, it becomes more difficult to drill through this type of formation. This will lead to additional casing strings being required to drill through this type of formation and ultimately to additional costs. Areas where this type of narrow mud window is prone to occur are; deep water drilling, drilling through depleted zones and lastly drilling through abnormal geopressured zones. A typical narrow mud window is shown in Figure

1.2

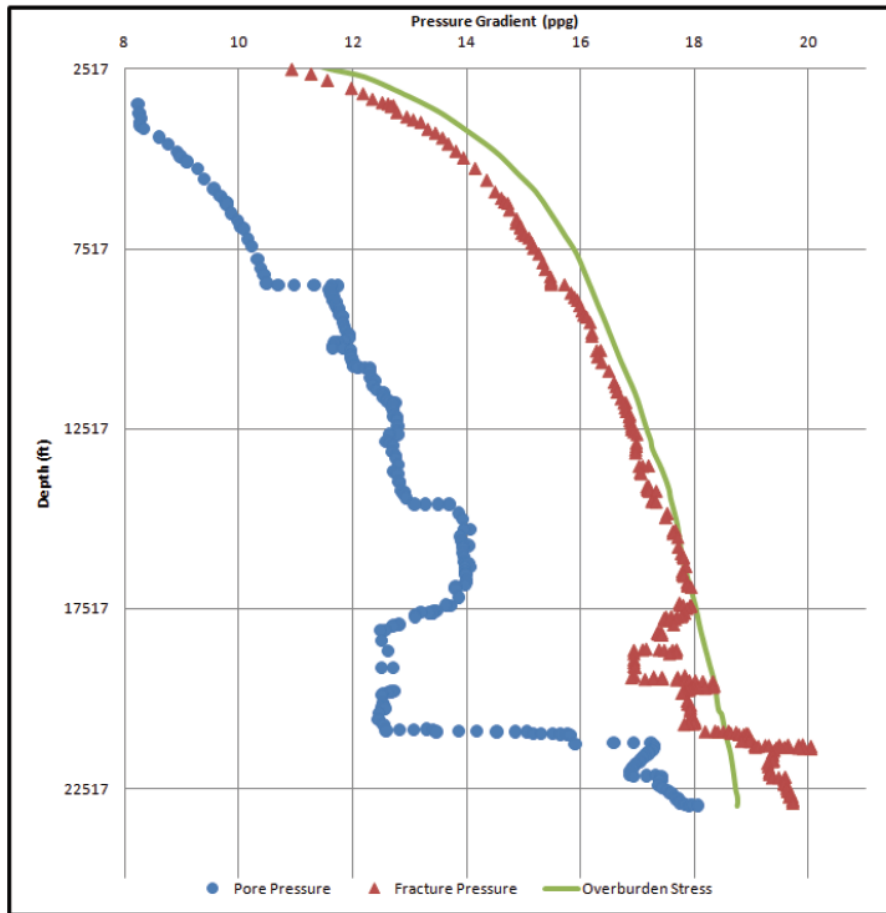


Figure 1.2: Typical narrow mud weight window⁴

The fracture gradient is obtained by determining the pressure at which losses begin to occur in the hole section and converting the pressure down hole to equivalent mud weight. One of the major advantages of wellbore strengthening is in assessing reserves in depleted zones and deep water drilling where the drilling window between pore pressure and fracture gradient is very narrow.

1.1.2 Fracture breakdown pressure prediction

Formation pore pressure is the pressure exerted by the fluid(s) in the pores of the rock formation while hoop stresses are stresses acting around the circumference of the wellbore caused by distortion of in-situ stresses by drilling operation. The fracture breakdown pressure (P_{fb}) for non-porous rock with anisotropic stresses is predicted using equation 1.1⁹:

$$P_{fb} = 3\sigma_h - \sigma_H + T_0 \quad 1.1$$

Porous rock fracture breakdown pressure (P_{fb}) is predicted by accounting for poroelasticity in two ways. The first case, when there is filter cake sealing with no communication between the pressure in the wellbore and the pressure in the formation, is given by equation 1.2⁹:

$$P_{fb} = 3\sigma_h - \sigma_H + T_0 - P_0 \quad 1.2$$

The second case, where there is no filter cake sealing and the pressure in the wellbore penetrates the formation, is given by equation 1.3⁹:

$$P_{fb} = \frac{3\sigma_h - \sigma_H + T_0 - \eta P_0}{(2 - \eta)} \quad 1.3$$

$$\text{Where } \eta = \frac{1-2\nu}{2(1-\nu)} \alpha$$

The poroelastic constant (η) in equation 1.3 above is always less than 1 thereby reducing the fracture breakdown pressure. This supports the fact that a sealing, isolating wellbore pressure from formation pressure is necessary for an increase in fracture breakdown pressure.

1.2 Literature review

Wellbore strengthening is simply the engineering practice of increasing the formation fracture gradient/resistance thereby increasing the width of the mud weight window or the widening of the gap between the pore pressure and fracture gradient of the formation. This allows the Driller to have better control of the Equivalent Circulating Density (ECD) of the mud which ultimately

leads to the mitigation of lost circulation and wellbore stability problems. It has been used for over a generation now to successfully prevent lost circulation by mixing lost circulation materials (LCM) particulate to drilling mud. The background experiments, general mechanisms involved, and review of previous works on wellbore strengthening are presented in this section. A brief introduction to Nano-particles, a key part of this work, will also be presented here.

1.2.1 DEA 13 experiments

The DEA 13 experiments conducted in the early 1990's were the earliest experiments performed to understand the mechanism of wellbore strengthening and form the basis for the widely accepted stress cage and fracture closure stress theories. Morita, Black and Fuh⁵ conducted hydraulic fracture laboratory tests using cubic 30x30x30 inches Berea sandstone with a 1.5 inches diameter borehole drilled at the center. 10 ppg and 16 ppg water based, mineral oil based and diesel based muds were used with the mud injection rate set at 0.5 cc/sec. Results showed that solids from drilling fluid seal the fracture inlet aperture resulting in a stable fracture and fracture breakdown occurs only when drilling fluid begins to enter the fracture. A narrow fracture tip zone exists which does not allow fluid invasion with a dehydrated mud zone behind the tip. Laboratory results gave abnormally large borehole breakdown pressure when compared to field findings. Lost circulation was revealed to depend on Young's modulus, wellbore size, mud solid bridging at fracture tip and the dehydrated zone with thermal cooling also having some effect.

Onyia⁶ carried out 35 hydraulic fracture experiments to determine fracture initiation and propagation pressures. Low (10 lbm/gal) and high (16 lbm/gal) density water based, diesel based and mineral based drilling muds were tested using Berea, Torrey Buff sandstone (30 in. cubes) and Mancos shale (20.5 in. cubes) cores with predrilled boreholes. Re-opening pressure tests

were performed 20 minutes and 1 hour after shut in to test the mud healing effect. LCMs tested were calcium carbonate and flake-type material. Results showed that there was no significant difference between breakdown pressure of water based and oil based mud except in the propagation and re-opening pressures. Fracture healing in water based mud is observed through saw tooth propagation characteristics caused by mud out sealing while the absence of this phenomenon in oil based mud showed the absence of fracture healing in oil based mud. Absence of saw tooth characteristics also indicates that there is little or no spurt loss from the fracture to the formation. Oil based mud fracture propagation is very unstable and difficult to control as only minimal change in wellbore pressure propagates the fracture. Oil based mud fracture propagation can be made to behave like water based mud by increasing its fluid loss capability. Permeability is needed for spurt loss which creates mud out and sealing filter cake in fracture. Re-opening pressure always approaches the fracture propagation pressure and it was also noted that calcium carbonate and diatomaceous earth LCMs give the best result for oil based mud. Figure 1.3 illustrates fracture growth in water and oil based muds while Figure 1.4 illustrates the saw tooth characteristics showing the breakdown pressure in water based mud.

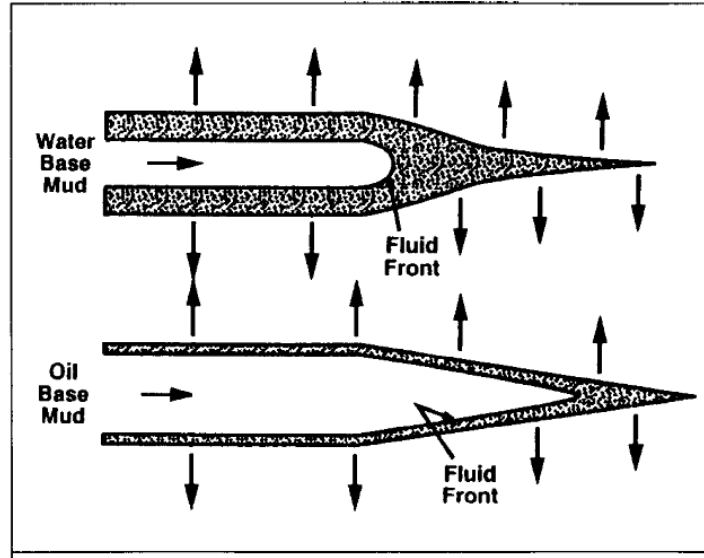


Figure 1.3: Fracture growth in water based and oil based mud⁶

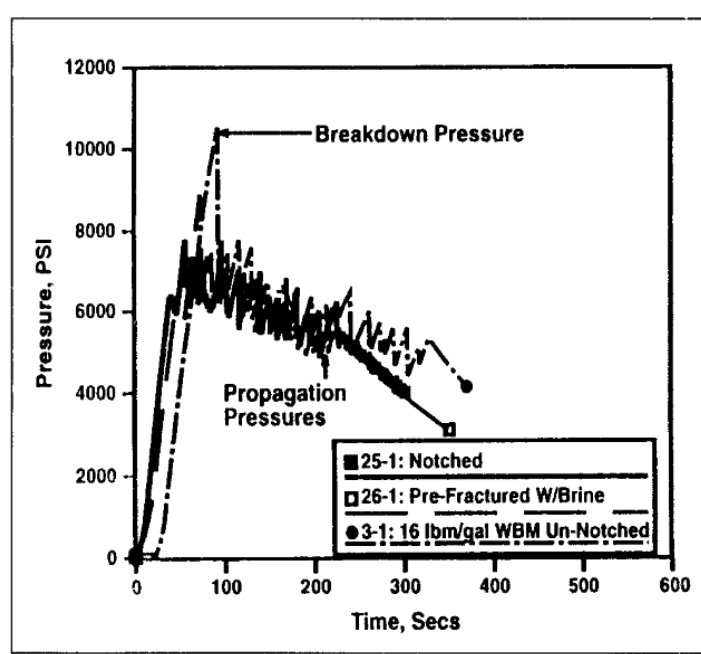


Figure 1.4: Fracture propagation saw tooth characteristics in water based mud⁶

1.2.2 GPRI experiments

Oort, Friedheim, Pierce and Lee⁷ reported that the GPRI joint-industry-project (JIP) investigation was a follow up to the DEA experiments carried out on a smaller scale to be able to test the

effectiveness of different types of LCMs in a cost effective manner. Results from the DEA experiments were confirmed and after testing a large number of LCMs in synthetic based mud, it was concluded that synthetic graphite of a specific type and size gave the most effective result.

1.2.3 Wellbore strengthening mechanisms

1.2.3.1 Stress cage

Alberty and Mclean⁸ proposed a physical model to explain the mechanism involved in fracture resistance increase by LCMs called the “stress cage” wellbore strengthening mechanism. It is simply a near wellbore region of high stress induced by propping open a shallow fracture and sealing it with additives at or near the wellbore/formation interface. The principle behind this model is that a newly formed fracture is propped open and sealed at the wellbore by solid additives. This effectively isolates the wellbore pressure from the fracture pressure. The permeable formation then allows the isolated fluid in the fracture, which is behind the blockage, to dissipate into the formation. The pressure in the isolated fracture then dissipates ultimately to the formation pore pressure leading to the fracture attempting to close behind the blockage. This creates a compression at the blockage which in turn increases the hoop stress value more than it was before carrying out stress caging. The induced fracture width, proppant particle size distribution, borehole diameter, formation permeability and mud sealing properties are significantly influential factors in stress caging. Model results showed that the magnitude of stress formed is dependent on formation toughness, width of fracture, where the blockage is formed within the fracture, length of fracture and compressive strength of the sealing/bridging material. The stress cage mechanism concept is illustrated in Figure 1.5.

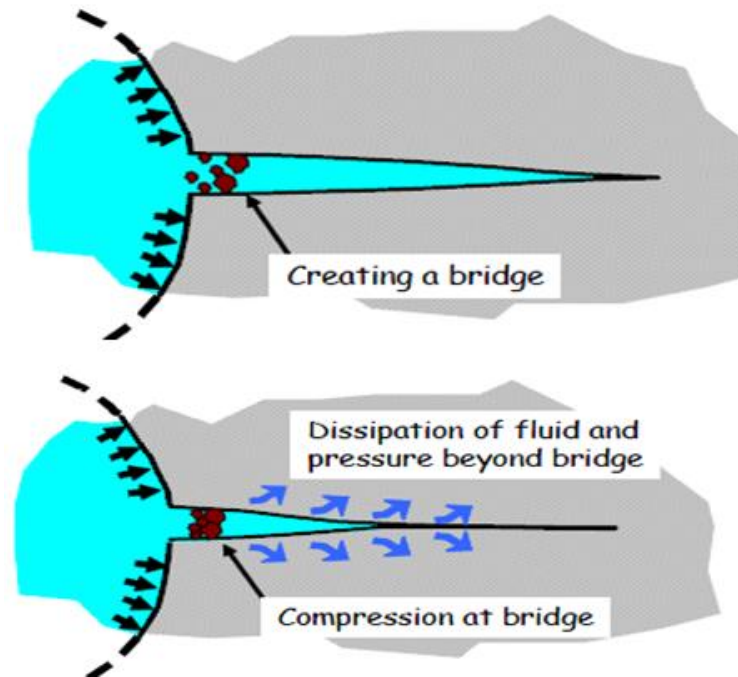


Figure 1.5: Stress caging mechanism⁸

1.2.3.2 Fracture closure stress

An alternative wellbore strengthening mechanism called fracture closure stress (FCS) was introduced by Dupriest³ in 2005, defining FCS as the stress holding the fracture faces closed. This stems from the idea that fracture width will continue to widen as the fracture grows and fluid loss will continue to occur as long as the equivalent circulating density (ECD) of the mud is greater than the FCS of the formation. This means that loss cannot be stopped by just plugging/bridging a fracture aperture with a particular size of LCM because the fracture width will continue to grow. LCM must continuously block and isolate the fracture tip as the fracture widens more than the particulate diameter. This then implies that a LCM should have the ability to prop open the width of a fracture at the wellbore until the FCS of the formation is greater than the ECD of the mud, which is exposed to the fracture. The LCM then subsequently loses its carrier fluid to form an immobile mass that will effectively isolate wellbore pressure from the

fracture pressure. The effect of the closing fracture increases the tangential stress, thereby effectively increasing the fracture gradient/resistance. Contrary to the stress cage concept, this report concluded that LCM type, size or compressive strength is not important but rather the development of an immobile mass in the fracture is the key to wellbore strengthening. Other conclusions were that materials less than 100 microns cannot be used as LCMs since they will block the pore throats and prevent leak off of carrier fluid into the formation. Specialty products that do not require leak off should be applied in impermeable formations like shale, for wellbore strengthening. One of the key differences between the FCS concept and stress cage concept is that the induced fracture is quickly plugged with the right sized LCM at or near the tip of the wellbore whereas the fracture is plugged close to the fracture tip, with any LCM size in FCS concept. After plugging the fracture tip in the FCS concept, the LCM is then squeezed into the fracture until it is packed all the way back to the wellbore/fracture opening thereby giving a continuous seal from the fracture tip to the wellbore/fracture opening. Figure 1.6 illustrates the FCS concept.

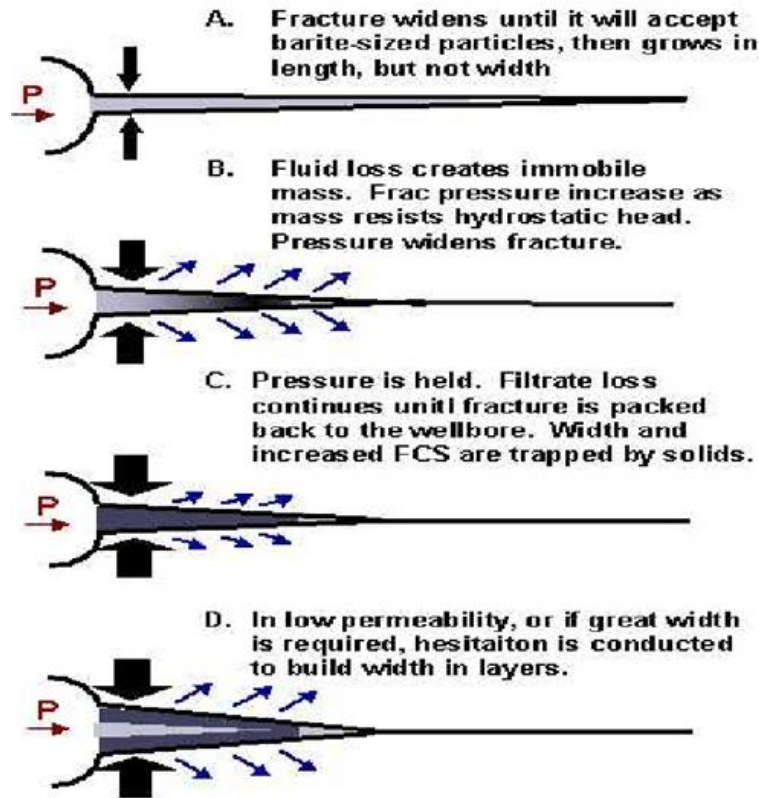


Figure 1.6: Fracture closure stress (FCS) mechanism³

1.2.4 Nano-particles

Nanomaterials are a good candidate for drilling fluid design because of their very good physio-chemical, thermal, electrical, hydrodynamic and interaction properties. A nano sized particle physically has dimensions equal to one billionth of a meter¹⁰. These very fine particles can gain easy access to the smallest of pores and pore throat, acting as very effective sealants to all types of formations including unconsolidated and shaly formations. The addition of nano-particles to drilling mud greatly improves its filtration properties forming a thin, non-erodible and impermeable filter cake. The resultant filter cake can also be easily removed before well

completion due to the huge surface area to volume ratio of the nano-particles which allows for extensive interaction with the mud. The sponge like clustering of nano-particles caused by high aggregation of surface area to volume ratio also make them very applicable to completion fluid design as this feature helps prevent fluid invasion and consequently formation damage¹¹. The key advantage nano sized materials have over micro and macro sized particles is their far greater surface area to volume ratio. This attractive property gives nano-particles unrestricted access to the finest of pore spaces of near wellbore formations and makes them particularly useful in: eliminating shale-mud interaction while drilling due to their high interaction potentials; improving thermal conductivity of drilling fluid which leads to bit cooling and high mobility; reducing wear and tear of down hole equipment due to its very low kinetic energy; preventing borehole instability and lost circulation problems due to their sealing and strengthening potentials. It is also environmentally friendly because only a very small quantity is needed for mud additives (typically <1%). Figure 1.7 shows a picture of nano-particles aggregating at a pore throat while Figure 1.8 and Figure 1.9 shows the particle size scale and surface area to volume ratio of same volume materials.

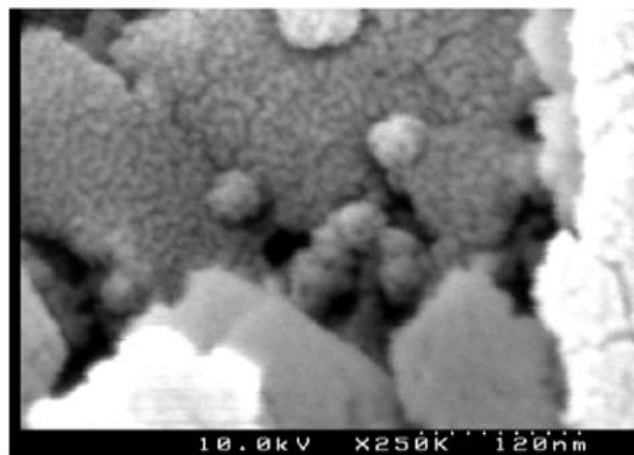


Figure 1.7: Showing aggregate of nano-particles plugging a pore throat¹²

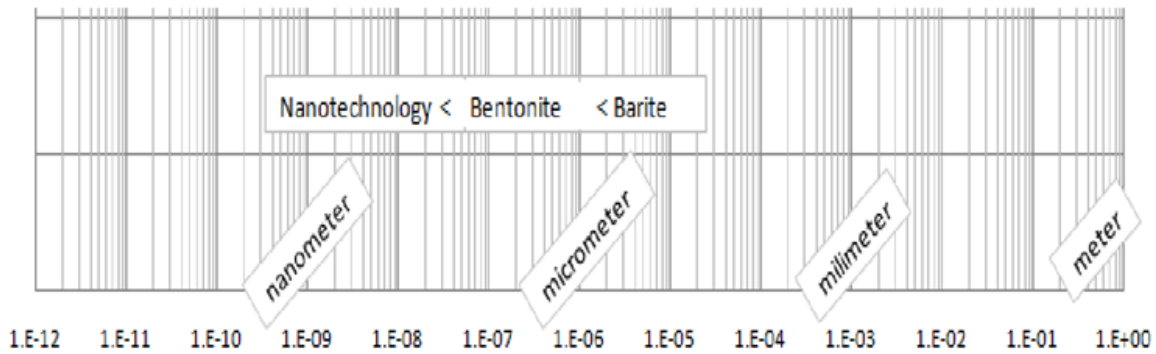


Figure 1.8: A particle size scale¹²

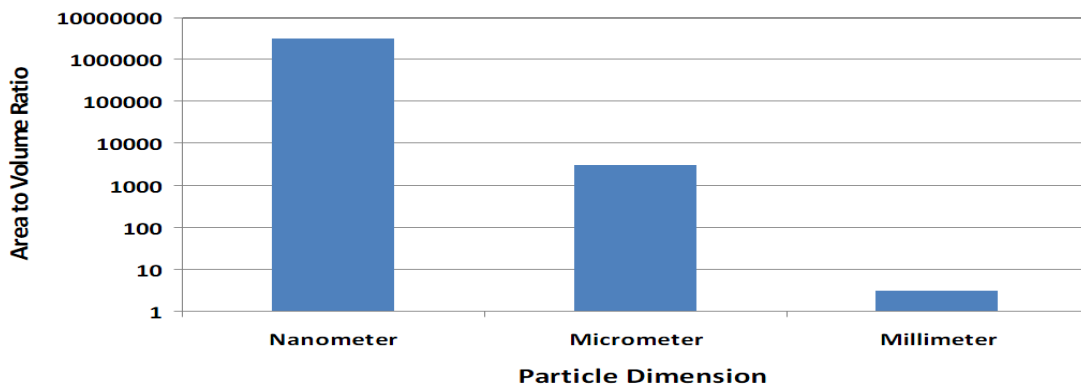


Figure 1.9: Surface area to volume ratio of same volume of materials¹¹

1.3 Research objectives

The main objectives of this project is to design a novel lost circulation material (LCM) blend by running hydraulic fracture experiments for both water based and invert emulsion (diesel oil) based muds and subsequently investigate the effectiveness of the designed LCM blend in an impermeable formation (concrete core). The LCM blend will comprise of nano-particles (in-house prepared) and regular granular LCMs with the optimum designed blend also giving moderate distortion in fluid rheology.

The unique, earlier highlighted qualities of nano-particles will be utilized in developing an optimum LCM blend capable of increasing fracture resistance/gradient substantially thereby

reducing lost circulation associated drilling costs. This approach is a novel one and at the time of writing this project there is no published literature yet on the combination of nano-particles and regular LCMs in drilling fluid LCM blend design. Based on literature findings of LCMs that give the best wellbore strengthening results, graphite and calcium are utilized in this work. These LCMs will be combined with two samples of in-house prepared nano-particles identified as NP1 and NP2 and used in running hydraulic fracture experiments in the lab. At the end of this work, the answers to the following questions are expected to be identified.

1. Is there any significant difference in the observed results between NP1 and NP2 combination with graphite?
2. Is there any significant difference in the observed results between the established optimum NP1 and NP2 blend with graphite when comparing the same optimum concentration blend using calcium carbonate LCM instead of graphite?
3. Is there any major difference in the observed results when comparing the established optimum blend in water based mud with the same optimum blend using invert emulsion (diesel oil) based mud?
4. Is there any significant difference between the optimum NP1 and NP2 blend for water based mud in sandstone and impermeable concrete cores?
5. Can we see the same result trends observed in sandstone cores using concrete core samples in order to confirm experiment repeatability?

The nano-particles (NP1, NP2) and granular particles (graphite, calcium) are set at high and low combination concentrations for the experiments. Each experiment run will blend set concentrations of nano-particles and granular particles which will be thoroughly mixed with the base mud. The blended mud will then be flowed through a hydraulic fracture apparatus

with a prepared core in place, pumping the mud into the core until it fractures. Re-opening pressure test will be carried out after 10 minutes of shut in time to assess the healing power of the blend. The fracture breakdown pressures will be analysed along with the mud rheology of each blend and based on the results, an optimum concentration blend will be established. Heterogeneity of sandstone cores will also be assessed by taking some rock property measurements.

The experiment is divided into three stages as follows:

1. Core sample preparation
2. Fracturing fluid preparation
3. Hydraulic fracture apparatus operation and data collection

Data collected will be analysed and interpreted with informed conclusions drawn based on the findings. Recommendations for future work, along with lessons learned, will also be presented.

Chapter Two: **EXPERIMENTAL DESIGN PARAMETERS AND HYDRAULIC FRACTURE APPARATUS SET-UP**

The experimental design parameters and hydraulic fracture set up will be introduced and discussed in this section.

2.1 Experimental parameters

It is necessary for the success of any experimental work to identify the key variables or parameters involved and categorise them accordingly. The parameters for this work are split into three categories as follows: uncontrollable, fixed and variable. The experimental design is modeled after a two way factorial design with two nano-particles, two granular particles and two concentration levels set at high and low. Interpretative analysis will then be used to draw final conclusions.

2.1.1 Uncontrollable parameter

The fracture width is not fixed or controlled for this experiment. Fracture is induced in the core and allowed to propagate simulating actual field behaviour of induced fractures while drilling.

2.1.2 Fixed parameters

For the purpose of this work, the following parameters relating to the hydraulic fracture apparatus operation are fixed as follows:

1. Core is cylindrical with geometry fixed at 5.75'' in diameter, maximum height of 9'' and 0.5'' borehole diameter.
2. Confining pressure is set at 100 psi
3. Overburden pressure is set at 400 psi
4. Testing temperature is room temperature
5. Injection rate is set at 5ml/min

2.1.3 Variable parameters

These are the parameters being varied throughout the experiments with the nano-particles and granular particles also set at fixed high and low concentrations.

1. Nano-particles – Two nano-particles samples (NP1 and NP2) prepared in-house were used for the experiments. NP1 is iron (III) hydroxide nano-particles while NP2 is calcium carbonate nano-particles, products of research work within the drilling research group at the University of Calgary.
2. Granular particles – Two granular particles (A and B) used regularly as LCMs in industry were used for the experiments. Granular particle A is graphite (glide graph) with particle sizes ranging from 70 microns to 220 microns. Granular particle B is calcium carbonate with particle sizes ranging from 10 microns to 250 microns.
3. Water based and invert emulsion based (diesel oil) drilling fluids were utilized for the experiments.
4. Sandstone and concrete cores were used for testing. The sandstone used was obtained from outcrops in a quarry in Jefferson City, mid-Missouri and is called Roubidoux sandstone while the concrete cores were prepared in the lab using basic uniform mortar mix.

2.2 Hydraulic fracture apparatus set up

The identification of the different components that make up the hydraulic fracture apparatus, their functions and knowledge of its data acquisition system is crucial to the success of any hydraulic fracture tests to be carried out. Maximiliano Lieberman's MSc thesis work¹³ from the Missouri University of Science and Technology will form the basis for the information presented here. The complexity of the system is illustrated with a detailed schematic in Figure 2.1.

The major components that allow the hydraulic fracture system to achieve its main goals of creating induced vertical/horizontal fractures using treated mud and accurate data capture are looked at in detail in this section. Figure 2.2 shows the hydraulic fracture apparatus.

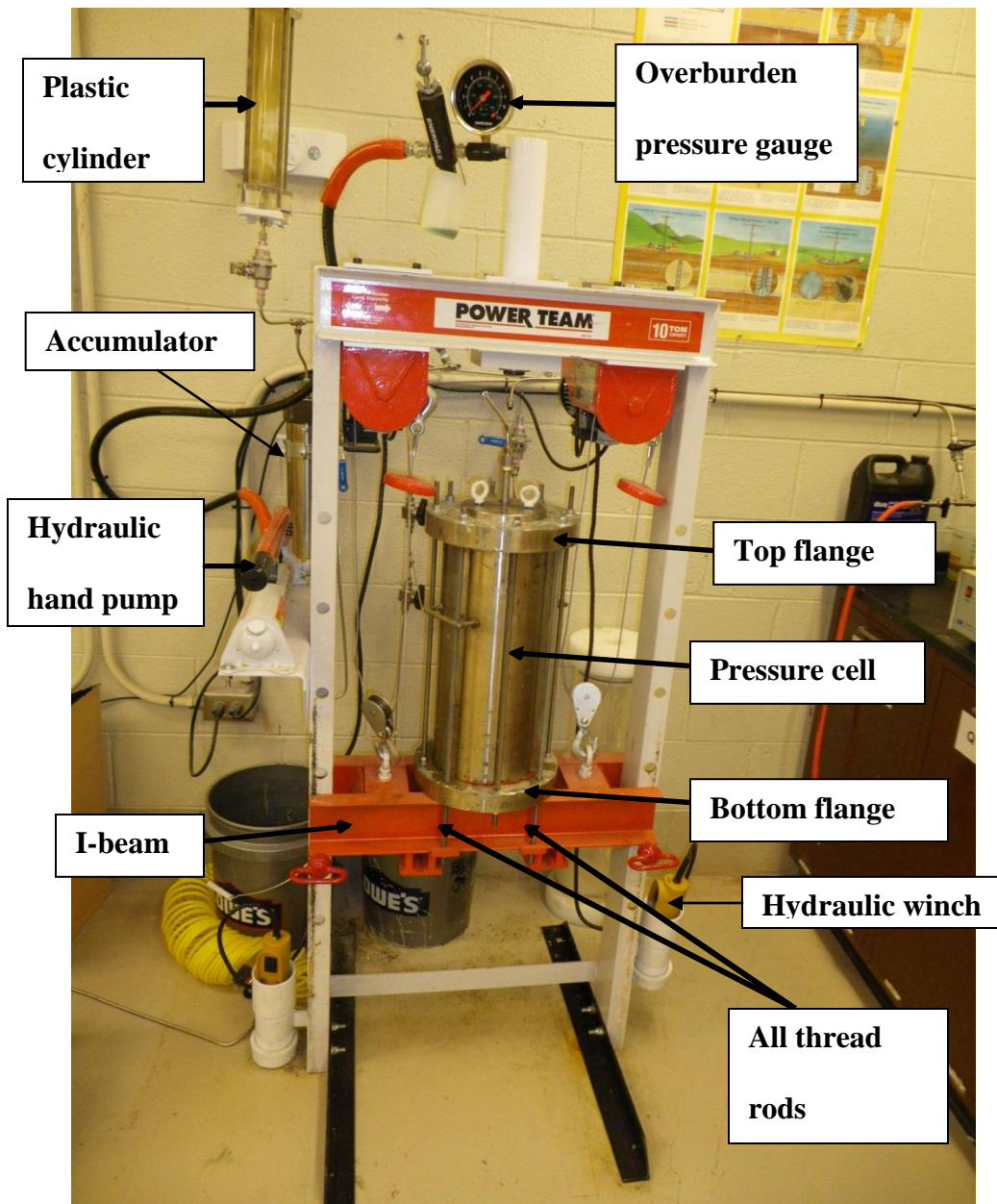


Figure 2.2: Hydraulic fracture apparatus

2.2.1 Pump system and fluid distribution

High pressure (10,000 psi), low volume (100ml) Isco DX100 syringe pumps are used to build and apply confining or injection pressure inside the hydraulic fracture apparatus. The fluid (water) with which these pumps operate is contained in a plastic or stainless steel container used as a reservoir. Each pump has an inlet valve that allows fluid to flow into the pump piston during refilling and discharging. The tubings that allow fluid distribution to and from the pumps as well as into the hydraulic fracture apparatus are 1/8'' and 1/4'' OD stainless steel. The outlet valve on each pump prevents the system from depressurizing while being refilled. Figure 2.3 shows the Isco DX100 syringe type pumps used for pumping fluid into the apparatus.



Figure 2.3: Isco DX100 syringe type pumps

2.2.2 Accumulator

A stainless steel pipe with an internal piston accumulates and injects fluid into the core sample. The accumulator is loaded with the desired drilling mud and then by means of injecting water beneath the piston, the mud is transferred and injected into the core sample. As can be seen from the schematic diagram in Figure 2.4, mud is transferred to the accumulator by filling a plastic cylinder and then applying compressed air to force the mud into the accumulator. Pressure is then built underneath the piston which displaces the mud into the core sample.

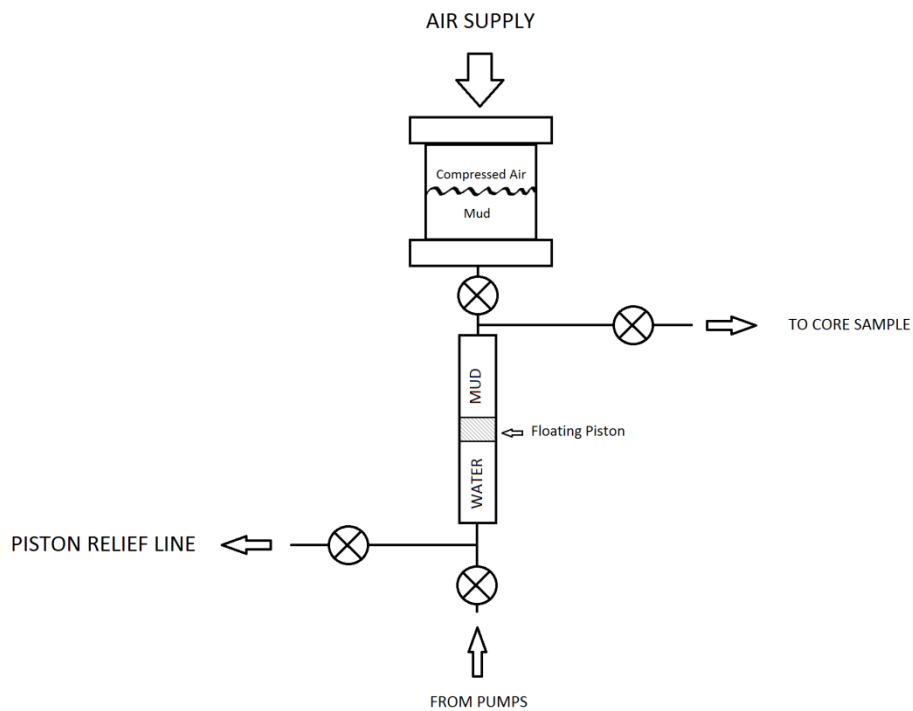


Figure 2.4: Mud accumulator system¹³

2.2.3 Hydraulic piston

The hydraulic “hand” pump is connected to a piston located on the top of the apparatus frame. The only function of this piston is to apply axial load onto the top cap which creates the overburden stress applied on the core. Figure 2.5 shows an illustration of how this works.

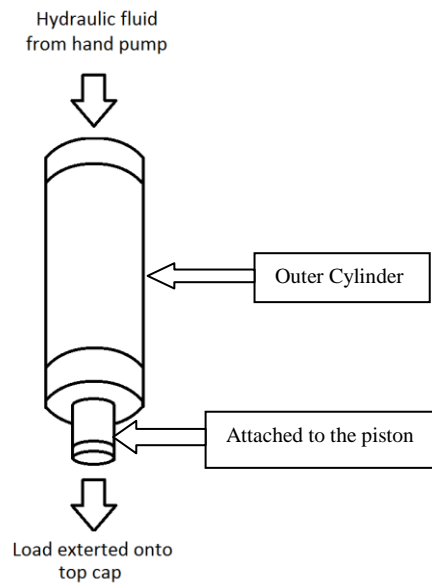


Figure 2.5: Overburden piston¹³

2.2.4 In-line pressure regulator

A pressure regulator as illustrated in Figure 2.6 is mounted in between the hand pump and piston. This is used to bleed off hydraulic fluid in cases when pressure inside the piston exceeds the desired pressure.

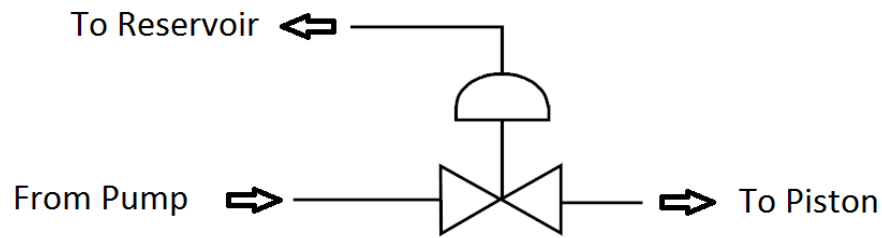


Figure 2.6: Bleed-off valve¹³

2.2.5 Rubber sleeve

This is used to apply confining pressure inside the hydraulic fracture apparatus. Pressure is built up in the gap between the stainless steel cylinder and the rubber sleeve, thus as pressure is increased the rubber sleeve applies pressure around the core until desired confining pressure is reached.

2.2.6 Stainless steel cylinder

The highly pressurized fluid used to apply confining stress around the core is contained by a pressure vessel called the stainless steel cylinder. This cylinder is placed over the rubber sleeve and rests on the bottom flange.

2.2.7 All thread rods

All six thread rods are mounted on the I-beam and are used to secure and clamp down the top flange onto the stainless steel cylinder. This creates a seal for the rubber sleeve preventing leaks from the confining chamber onto the upper section of the core sample.

2.2.8 Bottom flange

The bottom flange serves as the base and foundation of the hydraulic fracture apparatus. It is securely bolted onto the I-beam and serves as core holder while also supporting the stainless

steel cylinder and rubber sleeve. The rubber sleeve is glued with clear silicone onto the core holder to avoid leaks.

2.2.9 Top flange

The top flange rests on the stainless steel cylinder and rubber sleeve with an opening in the center to allow placement of cores into the apparatus. It provides a seal between the stainless steel cylinder and rubber sleeve, hence preventing confining pressure losses due to leaks.

2.2.10 Hydraulic fracture apparatus frame

The frame is the skeleton of the hydraulic fracture apparatus and serves as support for it. The bottom flange rests on the I-beam which is capable of moving up and down by means of two hydraulic operated winches. The hand pump, which drives the piston mounted on the top of the frame, is positioned at the left side of the frame. The frame is fitted with several holes that allow the I-beam to come to rest at different heights.

2.2.11 Data acquisition

The software provided by the pump manufacturer (Isco pump) is used to record the pressure at which the pump is injecting the fluid into the core sample. This software operates and records the pump parameters remotely from a computer. The pump controller is connected to an rs-232 serial port on the computer by a special serial cable provided by the pump manufacturer. This software stores the data generated from the pump but this data as it appears on the original file must be re-configured to allow the user to see the actual data. The factors used in this conversion can be found in the Isco pump manual. In addition to being able to record injection pressure from the pump, a pressure gauge is also installed on the injection line so as to be able to compare values and measure pressure head losses in the system.

Chapter Three: **EXPERIMENTAL PROCEDURES FOR HYDRAULIC FRACTURE OPERATION**

The hydraulic fracture operation experimental procedures are split into the following categories:

1. Core sample preparation.
2. Hydraulic fracture apparatus operation.
3. Fracturing fluid mixing.
4. Rock tensile strength measurement.

3.1 Core sample preparation procedure

The core sample preparation process is a very rigorous and engaging one. The procedures must be carefully adhered to at every stage. Each process impacts on the success of the next stage and ultimately to the core being placed without any issues in the hydraulic fracture pressure cell for testing. The following are the sandstone core preparation steps for the hydraulic fracture operation:

1. Collect rectangular core slabs from sandstone outcrop quarry.
2. Drill out cylindrical cores with 5 ¾” coring drill bit from rectangular core slab using the drill press.
3. Cut both sides of cylindrical core surface with slab saw. This cuts off the rough surface in preparation for surface grinding.
4. Grind the cut surface with surface grinder until a flat surface is achieved.
5. Drill a borehole in the center of the core with ½” drill bit using the drill press.
6. Fix cylindrical steel caps on either side of core using epoxy gel.
7. Vacuum core for 24 hrs in vacuum chamber to remove air from pores of core.

8. Run water into vacuum chamber and soak core for 3 hours to fully saturate rock pores with water and build up pore pressure, before placing core in pressure cell for testing.

The procedures for these steps are as follows:

3.1.1 Drilling out cylindrical cores

1. Grease thread on Drill press.
2. Fasten 5 3/4" cylindrical coring drill bit to Drill press using wrenches.
3. Secure slab firmly to work table.
4. Attach water hose to water inlet of drill press and open tap to the maximum to allow full water jet into the drill bit. This cools the bit while drilling and avoids stuck pipe issues.
5. Start drilling until drill bit goes all the way through the rectangular core slab.
6. Stop drilling, remove cut slab and repeat process until all cores have been cut from slab.
7. Using 2" coring bit, core out sample for tensile stress testing and porosity and permeability measurements.

3.1.2 Cutting core surface with slab saw

1. Place core on slab saw movable table and adjust core position until the blade of the slab saw aligns with the surface of the core. Ensure that the blade just barely cuts the surface to avoid cutting the sandstone too deep and making the length too short. Ideal core height should range from 7" to 9" before fixing steel caps.
2. Secure core firmly to movable table.
3. Fill tank supplying water to the slab saw cutter with water. This cools the blade of the slab saw while cutting cores by spraying water through the water outlet close to the blade.
4. Switch on the machine and check that water is spraying the blade from the water outlet.

5. Close the lid of the slab saw and wait for 20 minutes or until the cut surface falls off the core.
6. Repeat process for the other side of the core.

3.1.3 Grinding core using a surface grinder

1. Place the v-block on the movable table of the surface grinding machine.
2. Place the lever used to magnetize the v-block to the surface grinding machine down. This activates the magnet that holds the v-block firmly to the movable table.
3. Place the core against the v-block at any given height and fasten it tightly to the block.
4. Adjust the height of the grinding wheel of the surface grinder so that it barely touches the surface of the core.
5. Pour water into the water tank of the machine and turn on the water pump to start flowing water to the grinding wheel. This cools the grinding wheel while in operation.
6. Switch on the machine. This runs the grinding wheel and movable table.
7. Run wheel until core surface is smooth and square. Use the level bulb to check for flatness.
8. Flip core and place square face on a small v-block shaped metal block, leaving the rough surface free.
9. Run grinding wheel until surface is smooth and square
10. Rotate core placing smooth surface on small metal block and run grinding wheel until core surface is smooth.
11. Flip core and finish smoothening the rough part of the surface which was on the bottom.

3.1.4 Drilling borehole in core

1. Take a center finder and draw lines on the surface of the core to locate the center of the core. Where the lines intersect is the center of the core.
2. Secure core on the work table of the drill press
3. Attach a ½” drill bit to the drill press. Use a shorter drill bit to drill a seat for the longer drill bit. This is because the longer drill bit is difficult to control and will, due to vibration, go off the center while drilling.
4. Attach the longer 2” drill bit and drill through till the end.

3.1.5 Fixing steel caps to core

This step is carried out in order to prevent fluid from escaping the wellbore and causing overburden losses.

1. Use thread extractor and wrench to remove thread stuck in the cap holes after cutting off cemented core.
2. Seal around the thread of 1 ½” casing with a Teflon tape.
3. Screw this casing into one side of the steel cap.
4. Repeat steps 2 and 3 for the other steel cap.
5. Place the core on the steel cap with the casing on the steel cap fitting into the borehole in the core.
6. If the core circular surface does not align perfectly with the top/bottom caps, use a Dremmel tool to enhance and open up the borehole until caps are perfectly aligned with the core.
7. Scratch the steel caps and cap casing surfaces with sand paper of 120/150 grit to create rough surfaces that allow a good bonding between cap and core.

8. Prepare epoxy gel mixture by mixing the Sikadur 30 Hi Mod Gels 1:1 ratio.
9. Spread mixed epoxy gel generously on a steel cap and place this cap on triple C-clamps.
10. Place the core carefully on the steel cap rotating the core until it is perfectly aligned with the steel cap.
11. Clamp core down on steel caps in steps to ensure proper alignment.
12. Clean excess epoxy and leave it to cure for 24 hours.
13. Repeat steps 8 –12 for the other steel cap when cementing it to the other side of the core.

3.1.6 Vacuuming core

1. Place the core into the vacuum chamber and close the lid of the chamber.
2. Connect the vacuum pump to the vacuum chamber and switch on the pump.
3. Leave the pump on for 24 hours

3.1.7 Soaking core in water

1. With the vacuuming pumping machine still on, add water to the vacuuming chamber by immersing the water inlet pipe of the vacuum chamber into a container filled with water and opening the valve located on it, to allow water into the chamber.
2. Close the valve as soon as the core is completely immersed in water.
3. Leave core in vacuuming chamber with the pumping machine on for 3 hours before placing core in hydraulic fracture apparatus for testing.

3.1.8 Concrete core preparation

1. Place core moulder into a plastic bucket/container
2. Scoop cement into core moulder container, shaking and filling until moulder is filled up.
3. Fill up two 28 oz. containers with water and pour the water into the plastic bucket/container away from the cement in the core moulder.

4. Remove the core moulder and thoroughly mix cement with water using the cement mixer.
5. Place the metal core holder on a flat wooden plank and lubricate it thoroughly.
6. Pour mixed cement into metal core holder to fill $\frac{1}{3}$ of it.
7. Dip a metal rod into the poured mixture 12 times, and then tap it gently around the sides with a rubber hammer. This ensures pockets of air are removed from the concrete mixture.
8. Pour mixed cement again into the metal core holder until $\frac{2}{3}$ of it is filled and repeat step 7.
9. Pour mixed cement into metal container until it completely fills it and repeat step 7.
10. Use a flat metal plate to level cement mixture in metal core holder and leave to cure for 7 days.

3.2 Hydraulic fracture apparatus operation procedure

The following is the general procedure followed in carrying out the hydraulic fracture experiments (a detailed experimental procedure check list can be found on Appendix A.).

1. Empty the accumulator of all drilling fluid. This ensures that there is no mixture of the fresh drilling fluid with the drilling fluid previously used to run experiments.
2. Place O-ring on the bottom seating of the core holder. This prevents fracturing fluid from escaping the bottom of the wellbore into the pressure cell chamber.
3. Gently place the prepared core according to section 3.1, into the core holder or pressure cell.
4. Couple apparatus to core, close confining exit valve and open confining intake valve.
5. Apply overburden pressure until desired pressure (400 psi).
6. Fill up confining until desired pressure (100 psi).

7. Refill mud accumulator with desired mud.
8. Remove air from accumulator.
9. Open Isco pump software on computer.
10. Assign a name to project and click on the check mark on the screen to accept changes.
11. Connect pump to computer clicking on the connect arrow on the screen.
12. Check that pumps are completely filled and all the valves are in the required positions.
13. Click on 'record' on computer screen and start recording.
14. Start injecting fracturing fluid into core at 5ml/minute.
15. Stop injecting after fracture breakdown has occurred. This is observed when injection pressure drops sharply and confining pressure increases.
16. Depressurize the system and allow the fracture to heal for 10 minutes.
17. Start pumping second cycle until fracture break down occurs.
18. Stop recording.
19. Uncouple apparatus and fill up pumps.
20. Remove core and clean apparatus.

3.3 Fracturing fluid mixing procedure

1. Measured the desired volume of water and pour into mud mixer.
2. Weigh 30 g bentonite and pour into the mud mixer.
3. Mix thoroughly for 40 minutes.
4. Measure the required quantity of LCM granular particle and add to mud mixer.
5. Mix nano-particles slurry thoroughly for 5 minutes using blender.
6. Add desired quantity of nano-particle to mud mixer.

7. Add 0.1g of surfactant (dioctyl sulfosuccinate sodium salt) to mud mixer to ensure proper mixing of mixture.
8. Mix entire blend in the mud mixer for 10 minutes.
9. Measure mud density of the blended mud using mud balance.
10. Measure rheological properties (viscosity) of the blended mud using a viscometer.

The in-house prepared nano-particles (NP1- iron (III) hydroxide nano-particles, NP2-calcium carbonate nano-particles) were blended with granular particles (A-graphite, B-calcium carbonate) and mixed with the desired mud. These two variables were set at fixed high and low concentrations. The volume of the entire mud mixture used for one experiment run, is 500ml with nano-particles and granular particles quantities measured in terms of wt% of the entire mixture. Table 3.1 shows the set high and low concentrations for both nano-particles and granular particles while Table 3.2 shows the fracture fluid mixture recipe.

Table 3.1: Showing the concentration percentage level set for both Nano-particles (NPs) and Granular particles

| Nano-particles (NP1, NP2) | Granular particles (A, B) |
|----------------------------|---------------------------|
| Low (L) = 0.2wt% | Low (L) = 0.1wt% |
| High (H) = 2.0wt% | High (H) = 1.0wt% |

Table 3.2 : Showing the fracture fluid mixture recipe for water based mud

| Blend type | Bentonite | Water | NP1 | NP2 | Graphite(A) | Calcium carbonate(B) | Set cocn% |
|------------|-----------|---------|------|------|-------------|----------------------|--------------|
| Control | 30g | 470ml | - | - | - | - | - |
| Blend 1 | 30g | 468.5ml | 1ml | - | 0.5g | - | NP1(L), A(L) |
| Blend 2 | 30g | 455.5ml | 10ml | - | 0.5g | - | NP1(H), A(L) |
| Blend 3 | 30g | 464ml | 1ml | - | 5g | - | NP1(L), A(H) |
| Blend 4 | 30g | 455ml | 10ml | - | 5g | - | NP1(H), A(H) |
| Blend 5 | 30g | 468.5ml | - | 1ml | 0.5g | - | NP2(L), A(L) |
| Blend 6 | 30g | 467.5ml | - | 10ml | 0.5g | - | NP2(H), A(L) |
| Blend 7 | 30g | 464.ml | - | 1ml | 5g | - | NP2(L), A(H) |
| Blend 8 | 30g | 455ml | - | 10ml | 5g | - | NP2(H), A(H) |
| Blend 9 | 30g | 464ml | 1ml | - | - | 5g | NP1(L), B(H) |
| Blend 10 | 30g | 455ml | - | 10ml | - | 5g | NP2(H), B(H) |

The quantity of the blended nano-particles and granular particles are the same for the blends tested using the invert emulsion (diesel oil) based mud with the only difference being that the unblended oil based mud samples were not prepared in the lab but were test samples received from Bri- Chem Supply Limited, a drilling fluid company with operations in Calgary. The invert emulsion drilling fluid supplied is dark brown opaque in colour with a flash point of 94 degrees Celsius and a boiling point of (180-320) degrees Celsius. Table 3.3 shows the chemical composition of the supplied OBM.

Table 3.3: Composition of Bri-Chem's OBM

| Composition of OBM | Concentration (%) |
|------------------------|-------------------|
| Petroleum Hydrocarbons | <0.5 |
| Calcium Hydroxide | 1-5 |
| Calcium Chloride | 0 |
| Heavy Aromatic Naphta | <0.5 |
| Petroleum Distillate | 60-100 |

3.4 Rock tensile stress measurement procedure

1. Using a small saw slab cut the 2" diameter core samples from the different core slabs in 1" height.
2. Weigh the cut samples and measure the exact diameter and height using a Vernier calliper.
3. Set up apparatus (piston should just touch the load sensor).
4. Open Labview load log program on computer and connect to pump.
5. Enter name of test and start recording.
6. Apply load on piston by running pump.
7. Continue applying load until core sample fail/fractures at the middle.
8. Update load stress at which rock failed, and core geometry measurement on the rock mechanical test lab sheet, to obtain the tensile strength of the core.

The porosity and permeability of the core samples were received from the core analysis lab at the Missouri University of Science and Technology. These measurements were undertaken to assess

the homogeneity of the core samples used for this work. The ideal case would be to use core samples with the same porosity, permeability and tensile strength. But in reality it is almost impossible to have completely uniform cores/rocks. The permeability measured here is the absolute permeability of the core with the core flooded with brine of known viscosity²⁴. The summary of the rock properties of the different cores used for this work are presented in Table 3.4 below.

Table 3.4: Core rock properties

| Core Number | Liquid or Absolute Permeability K (md) | Porosity Ø (%) | Tensile strength (psi) |
|-------------|---|----------------|------------------------|
| Core 1 | 54.83 | 11.04 | 667.17 |
| Core 2 | 95.65 | 14.33 | 140.69 |
| Core 3 | 262.77 | 12.25 | 306.03 |
| Core 4 | 106.18 | 13.10 | 278.47 |

Chapter Four: **RESULTS AND DISCUSSION**

The primary goals of the experimental set up and conditions are to induce vertical fractures in cores and effectively seal these fractures with the fracturing fluid mixture. It is important to stress that due to the heterogeneity of the sandstone cores, occasionally both horizontal and vertical fractures are induced in the cores. The complete experimental results and analysis of this work will be presented in this chapter. The whole idea behind the experimental design is to first establish the fracture breakdown pressure (fbp) of the core using unblended mud called the “control sample”. Then run tests, blending nano-particles and granular particles at different set concentrations in order to establish their different fracture breakdown pressures. Lastly, determine the blend that gives the highest fracture breakdown pressure, or sealing, with minimal distortion in mud density/rheology. The following experimental strategy was adopted:

1. Determine the optimum blend for NP1 and NP2 nano-particles in combination with granular particle A (graphite) using water based mud (WBM).
2. Using the established optimum combination above, combine NP1 and NP2 with granular particle B (calcium carbonate) to see if there is any significant difference in the result. This will confirm the importance of granular particle types in the wellbore strengthening process.
3. Using the established optimum combination blend, run tests using invert emulsion (diesel oil) based mud (OBM). Based on the result, establish an optimum combination for OBM.
4. Using the established optimum blends and a random blend, run tests using concrete cores for WBM. Noticing similar trends using sandstone and concrete cores will confirm experiment repeatability.

5. Analyze the concrete test result to see applicability of blend in wellbore strengthening in shale formations.

A total of 18 experiments were run using the above experimental strategy to be able to answer convincingly the questions posed earlier in the research objectives of this work.

4.1 Water based mud (WBM) data analysis

The data results and analysis using WBM will be dealt with in this section. The different blends nomenclature will be repeated again for proper clarity in Table 4.1 below. NP1 represents Iron (III) hydroxide nano-particles (NPs); NP2 represents Calcium Carbonate NPs; A represents graphite; B represents calcium carbonate.

Table 4.1: Showing the blend type and set concentration (cocn) level

| Blend | NP1 | NP2 | A | B | Set cocn level |
|----------|-----|-----|---|---|----------------|
| Blend 1 | √ | | √ | | NP1(L), A(L) |
| Blend 2 | √ | | √ | | NP1(H), A(L) |
| Blend 3 | √ | | √ | | NP1(L), A(H) |
| Blend 4 | √ | | √ | | NP1(H), A(H) |
| Blend 5 | | √ | √ | | NP2(L), A(L) |
| Blend 6 | | √ | √ | | NP2(H), A(L) |
| Blend 7 | | √ | √ | | NP2(L), A(H) |
| Blend 8 | | √ | √ | | NP2(H), A(H) |
| Blend 9 | √ | | | √ | NP1(L), B(H) |
| Blend 10 | | √ | | √ | NP2(H), B(H) |

The control sample plot for WBM showing the fracture breakdown pressure and re-opening pressure is shown in Figure 4.1. While Figure 4.2 shows the fracture breakdown pressures for various WBMs including the control sample. Table 4.2 then shows the fracture breakdown pressures (fbp) and percentage (%) increase in breakdown pressures of blended drilling fluids (DFs) over unblended drilling fluid (DF) in tabular form.

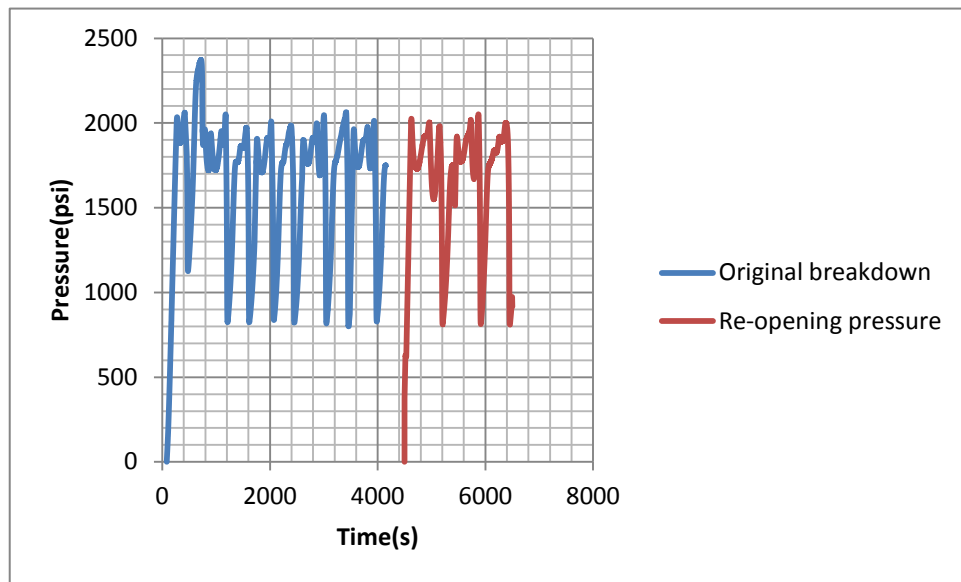


Figure 4.1: Plot showing original breakdown pressure and re-opening pressure of core using control sample for WBM

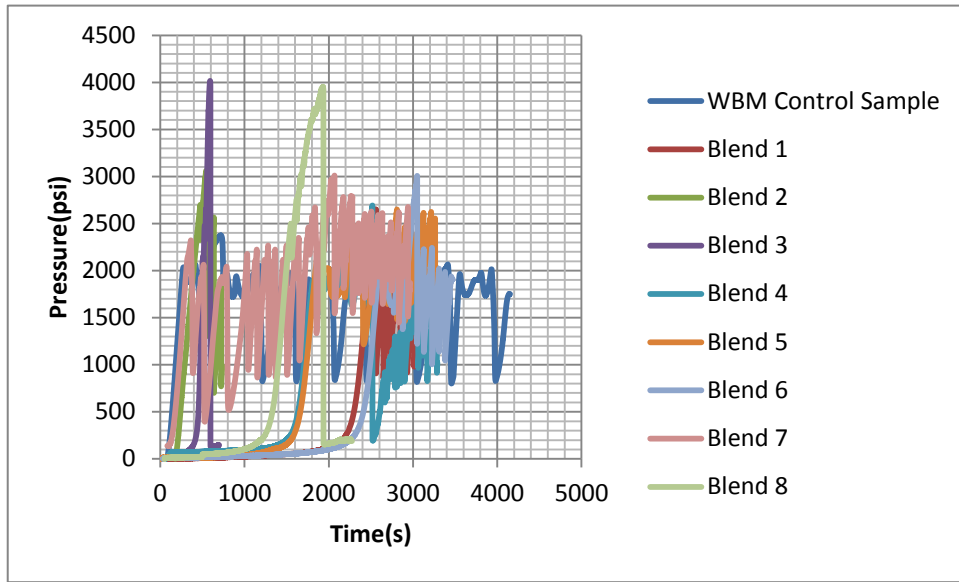


Figure 4.2: Plot showing fracture breakdown pressures (fbp) for various WBM blends

Table 4.2: Showing fbp and the % increase of fbp of blended DFs over unblended DF for WBM

| DF Type | Control | Blend 1 | Blend 2 | Blend 3 | Blend 4 | Blend 5 | Blend 6 | Blend 7 | Blend 8 | Blend 9 | Blend 10 |
|-----------------------|---------|---------|---------|---------|---------|---------|---------|---------|---------|---------|----------|
| fbp (psi) | 2,372.8 | 2,651 | 3,060 | 4,041 | 2,700 | 2,651 | 3,007 | 3,010 | 3,938 | 2,699 | 2,693 |
| Increase in fbp (psi) | - | 278.2 | 687.2 | 1,668.2 | 327.2 | 278.2 | 634.2 | 637.2 | 1,565.2 | 326.2 | 320.2 |
| % increase of fbp | - | 11.72 | 28.96 | 70.31 | 13.79 | 11.72 | 26.73 | 26.85 | 65.96 | 13.75 | 13.49 |

After completing the first round of experiments, the following observations were made from the results.

1. When combining iron (III) hydroxide nano-particles (NP1) with graphite (A), blend 3 gave the best results by far, with the highest increase in fbp.
2. When combining calcium carbonate nano-particles (NP2) with graphite (A), blend 8 gave the best results by far, with the highest increase in fbp.
3. Combination of NP1 and A gave poor results when both variables were set at high concentrations (blend 4).
4. Combination of NP2 and A gave similar results for blends 6 and 7.
5. Only a small increase in fbp was achieved when the variables were set at low concentrations (blends 1 and 5).
6. Testing the blends that gave the best results for both NP1 and NP2, i.e. blends 3 and 8 but this time substituting the graphite with calcium carbonate LCM, gave poor results. Only minimal fbp was achieved. This test confirms that LCM type is important in wellbore strengthening and that graphite gives a far better result than calcium carbonate in this respect. Figure 4.3 shows a plot of optimal blends using graphite and the same optimal blends concentrations using calcium carbonate.

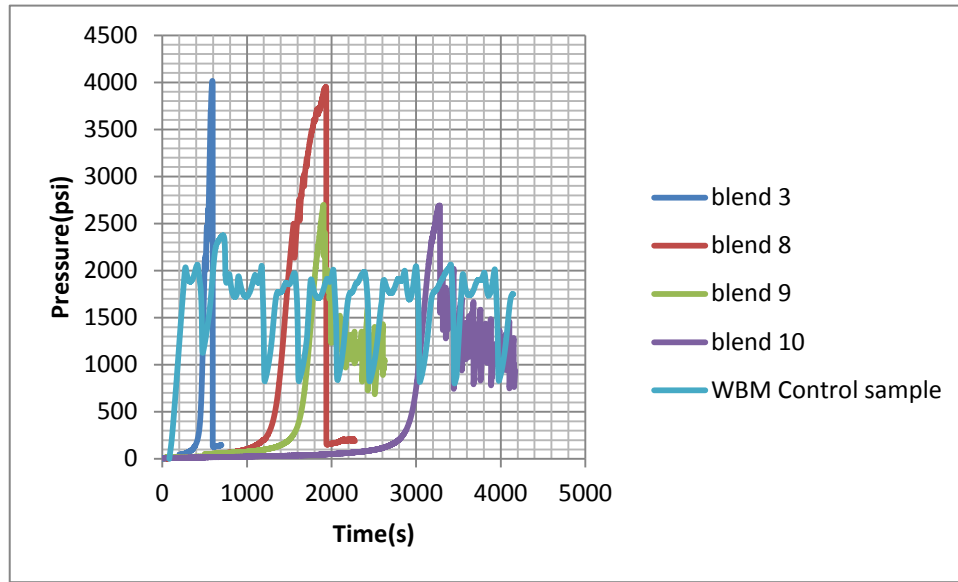


Figure 4.3: Showing optimal blends of NP1 and NP2 in combination with graphite and the same optimal blends in combination with calcium carbonate

The next stage of this analysis was to determine the optimal blend for WBM based on not just the blend that gave the highest increase in fbp but also considering the mud rheological properties. The blend that gives considerable increase in fbp with minimal distortion to the original/control mud will be the optimal/ideal blend. Table 4.3 shows the mud density and mud rheological properties for all blends including the control sample.

Table 4.3: Mud density and rheological properties of various WBM blends

| DF Type | Control | Blend 1 | Blend 2 | Blend 3 | Blend 4 | Blend 5 | Blend 6 | Blend 7 | Blend 8 | Blend 9 | Blend 10 |
|---|---------|------------|------------|--------------------|------------|------------|------------|------------|--------------------|------------|-------------|
| Mud Density (lb/gal) | 8.8 | 6.1 | 6.5 | 6.0 | 6.6 | 6.4 | 6.2 | 6.4 | 6.1 | 6.0 | 6.1 |
| Plastic Viscosity (cp) | 10 | 8 | 7 | 24 | 8 | 10 | 4 | 22 | 23 | 15 | 7 |
| Yield Point (lb/ ft ²) | 10 | 26 | 51 | 28 | 55 | 22 | 44 | 40 | 54 | 30 | 41 |
| 10 sec gel strength (lb/100ft ²) | 9 | 16 | 33 | 28 | 38 | 20 | 38 | 41 | 48 | 28 | 39 |
| 10 min gel strength (lb/100ft ²) | 20 | 24 | 34 | 39 | 38 | 25 | 52 | 64 | 66 | 36 | 59 |

The following key observations and deductions were established after considering the rheological properties of the different mud blends.

1. Blend 3 is established as the optimal blend for WBM as it gave the highest increase in fbp with minimal distortion in mud rheological properties as can be seen from Table 4.3 above.
2. Blend 8 will be the optimal blend if calcium carbonate NPs must be used instead of Iron (III) hydroxide nanoparticles for any operational/cost reason.
3. It was noticed after careful examination of the rheological properties results in Table 4.3 above that plastic viscosity and 10 min gel strength were very good signals or indicators that the fbp was going to increase significantly. When combining NP1 with graphite, blend 3 recorded the highest plastic viscosity and 10 min gel strength. Also when combining NP2 with graphite, blend 8 recorded the highest plastic viscosity and 10 min gel strength. Looking closely at these rheological properties will give an indication of how successful the fracturing fluid will be in wellbore strengthening.
4. These measurements also confirm what has been reported in many literatures that mud density does not have any impact on wellbore strengthening results.

Figure 4.4 shows a typical NP1 blend and Figure 4.5 shows a typical NP2 blend. A fractured core with both vertical and horizontal fractures due to rock heterogeneity is shown in Figure 4.6 while Figure 4.7 shows the cross section of a fractured core with the fracturing fluid leak off effect evident.



Figure 4.4: A typical NP1 blend in a mud mixer



Figure 4.5: A typical NP2 blend in a mud mixer



Figure 4.6: Fractured sandstone core showing both vertical and horizontal fractures



Figure 4.7: Cross section of fractured core showing the leak off effect

4.2 Oil (Diesel) based invert emulsion mud (OBM) data analysis

Continuing with the experimental strategy, the established optimal combinations of both NP1 i.e. blend 3 and NP2 i.e. blend 8, will be tested using invert emulsion (diesel oil) based mud (OBM) in an attempt to establish an optimal combination for OBM. A brief comparison between OBM and WBM with regard to the observed wellbore strengthening results will then be undertaken. Figure 4.8 shows the fracture breakdown pressures (fbp) for invert emulsion (diesel oil) mud (control sample) and fbp using blends 3 and 8. Table 4.4 shows fbp and the percentage increase in fbp of blended inverts over unblended invert mud. While the mud rheological properties are shown in Table 4.5.

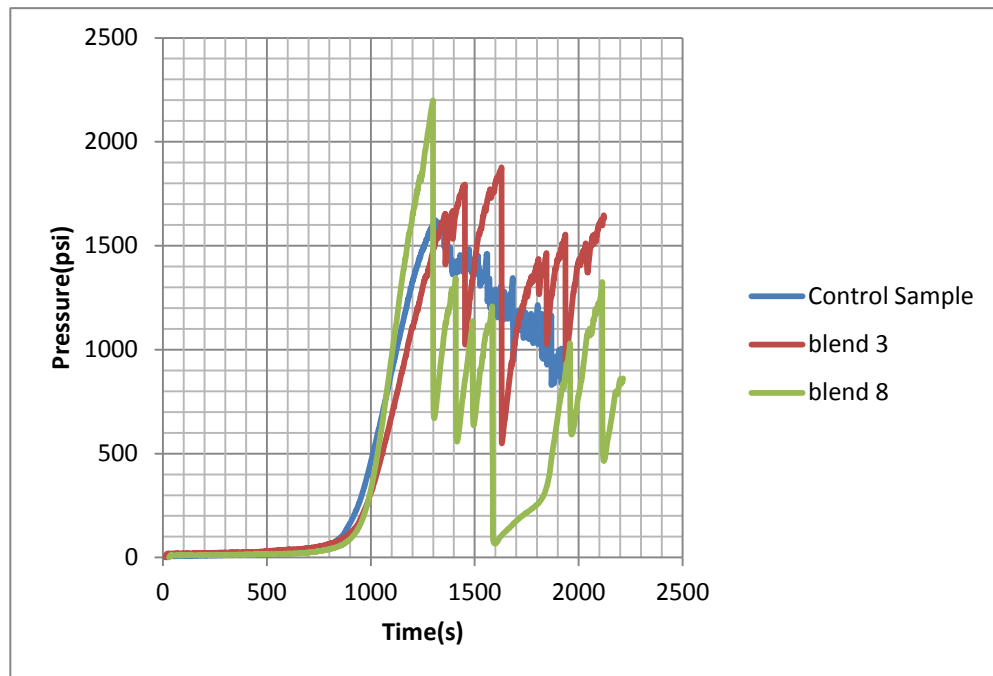


Figure 4.8: Plot showing fbp for invert emulsion (diesel oil) mud using established optimal blends 3 and 8

Table 4.4: Showing fbp and % increase of fbp of blended inverts over unblended invert DF

| DF Type | Unblended Invert DF | Blend 3 | Blend 8 |
|-----------------------|---------------------|---------|---------|
| fbp (psi) | 1,612.6 | 1,878.0 | 2,199.4 |
| Increase in fbp (psi) | - | 265.4 | 586.8 |
| % increase in fbp | - | 16.46 | 36.39 |

Table 4.5: Showing rheological properties of invert (diesel oil) based DF blends

| DF Type | Unblended invert DF | Blend 3 | Blend 8 |
|--|---------------------|---------|---------|
| Mud Density (lb/gal) | 7.65 | 7.7 | 7.4 |
| Plastic Viscosity (cp) | 22 | 23 | 32 |
| Yield Point (lb/ ft ²) | 3 | 5 | 14 |
| 10 sec gel strength (lb/100ft ²) | 2 | 2 | 6 |
| 10 min gel strength (lb/100ft ²) | 3 | 4 | 12 |

Based on the graphical and tabular results presented above, blend 8 is the optimal blend for invert emulsion (diesel oil) based mud. The increase in fbp for blend 8 is almost twice as much as the fbp increase recorded for blend 3. The rheological properties of blend 8 also shows a slight distortion in rheological properties which is well compensated for with the substantial increase in fbp. Figure 4.9 shows a typical invert emulsion (diesel oil) based mud (OBM) blend while a vertically fractured sandstone core using OBM is shown in Figure 4.10.



Figure 4.9: Typical OBM blend

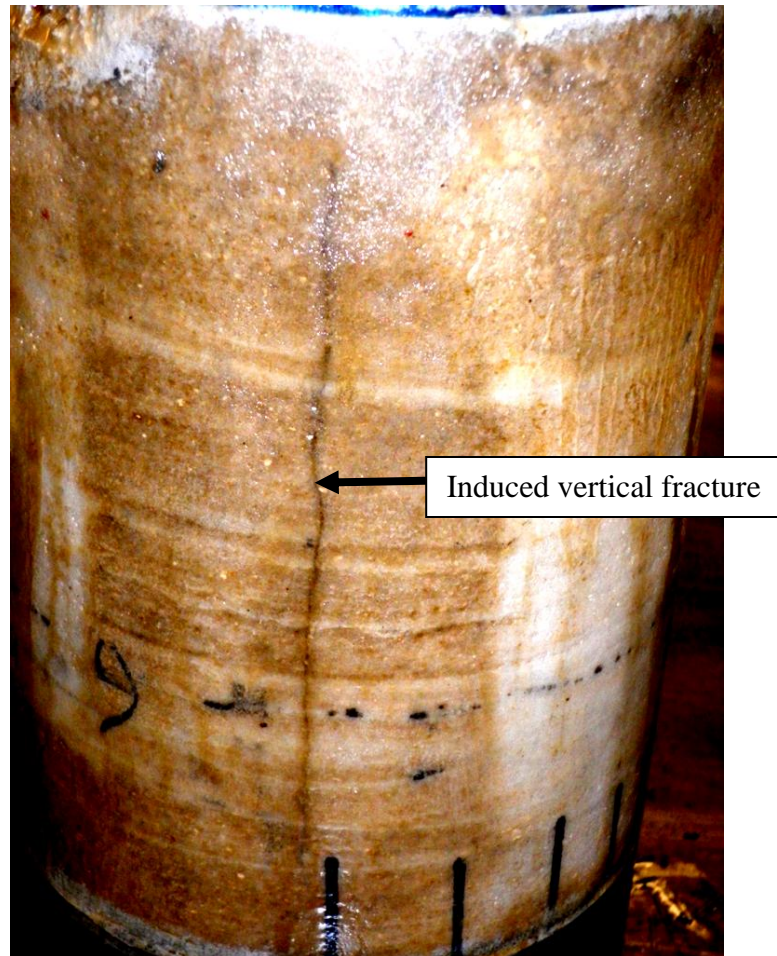


Figure 4.10: Vertically fractured sandstone core using OBM blend

4.3 Observed differences in fracture breakdown pressures (fbp) between invert emulsion (diesel oil) based mud (OBM) and water based mud (WBM)

It is pertinent to compare and contrast the observed results between the OBM and WBM used for this work in order to be able to better improve results from the OBM established optimal blend. As noted earlier in the literature review section, it is very difficult to achieve wellbore strengthening using OBM because of the absence of fracture healing in OBM observed through the absence of the saw tooth characteristics in the pressure profile plot. This indicates little or no spurt loss to the formation resulting in the fracture propagation being very unstable and difficult to control. Onyia⁶ concluded that using low (10 lbm/gal) and high (16 lbm/gal) density water based and diesel oil based mud that there is no significant difference between fbp of WBM and OBM except in the propagation and re-opening pressures. Contrary to this conclusion, the results of this work show that there is a significant difference in the fbp between the low OBM (7.7 lb/gal) and low WBM (8.8 lb/gal) used in this work. The results of this project also confirm the work by Onyia⁶ that OBM can be made to behave like WBM in terms of wellbore strengthening by adding fluid loss agents which consequently increase the fluid loss capability of the OBM thereby enhancing the leak off effect into the surrounding formation. This is further confirmed with the impermeable core tests showing the importance of permeability in wellbore strengthening, highlighting the need for fluid leak off into the surrounding formation which releases the pressure in the fracture and ultimately leads to fracture closure. Figure 4.11 shows the differences in fbp of OBM and WBM control samples while Table 4.6 shows the significant difference in fbp of the control samples. Figure 4.12 shows the differences in WBM optimal blend and the same blends using OBM.

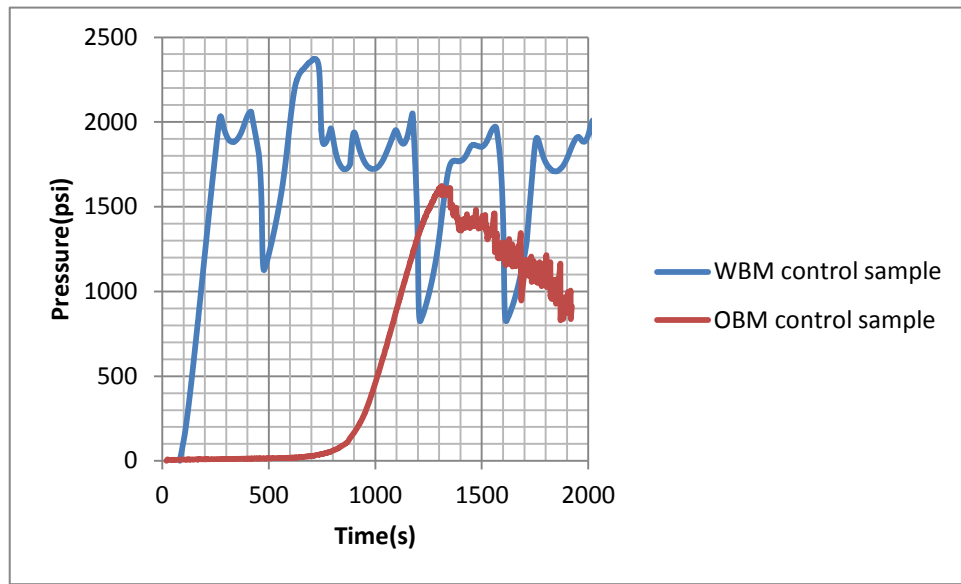


Figure 4.11: Showing differences in fbp between WBM and OBM control samples

Table 4.6: Showing significant differences in OBM and WBM control samples fbp

| DF Type | OBM | WBM |
|---------------------------|---------|---------|
| fbp (psi) | 1,612.6 | 2,372.8 |
| Difference in fbp (psi) | - | 760.20 |
| Percentage difference (%) | - | 47.14 |

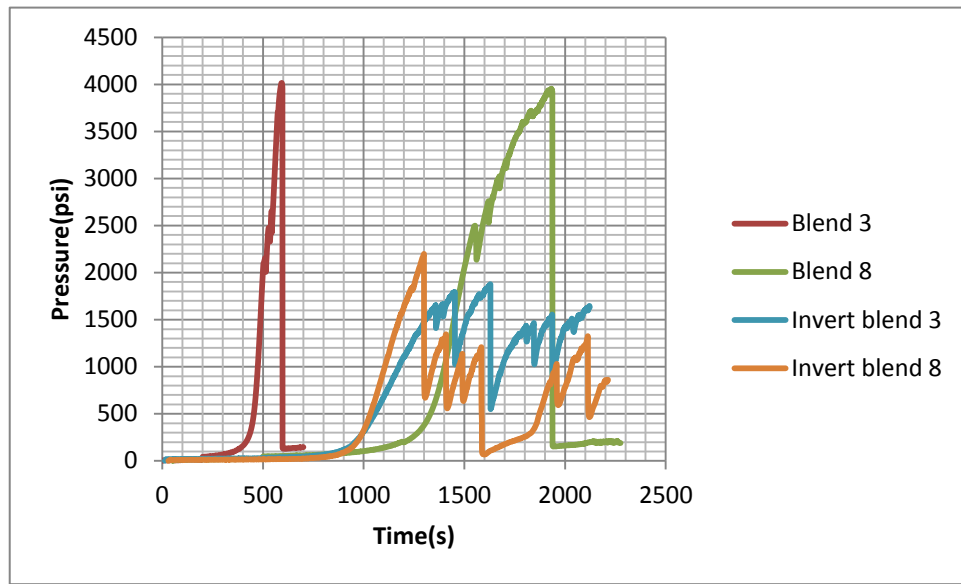


Figure 4.12: Showing the fbp of optimal WBM blends and fbp of the same blends in OBM

4.4 Concrete test data analysis (Impermeable formation test)

Due to the heterogeneity of sandstone cores and the inherent errors in result analysis this might pose, it became necessary to carry out tests using concrete cores to confirm repeatability of results. The concrete cores as prepared in Section 3.1.8 were made with the same material mixed in exactly the same proportion to ensure that all the concrete cores are completely homogenous. The tests with the concrete cores also give an indication of how well the WBM optimal blends strengthen the wellbore in completely impermeable formation, showing its applicability in wellbore strengthening in shale formations which is not 100% impermeable, like concrete cores. A control sample using WBM was first tested on the concrete core to establish the fbp of the concrete core. Blends 3 and 8 were then used to induce fractures on the concrete cores with blend 9 used as a random blend also in inducing vertical fractures. The goal was to check for the same trend in results as observed in sandstone cores which will effectively confirm the repeatability of results while also indicating how much fbp increase can be achieved. Figure 4.13 shows a plot of

the fbp using the different blends while Table 4.7 shows the fbp of the different blends and the percentage increase in fbp achieved for the different blends.

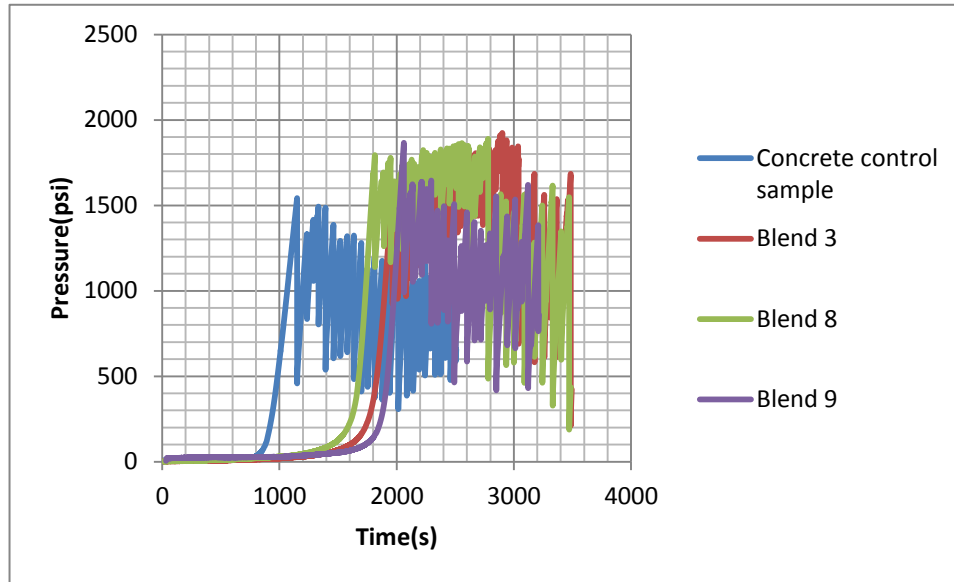


Figure 4.13: Showing fbp of different blends using concrete cores

Table 4.7: Showing the fbp of different blends and the % increase in fbp achieved in concrete cores

| DF Type | Control | Blend 3 | Blend 8 | Blend 9 |
|-----------------------|---------|---------|---------|---------|
| fbp (psi) | 1,543.2 | 1,923.4 | 1,889.6 | 1,867.0 |
| Increase in fbp (psi) | - | 380.2 | 346.4 | 323.8 |
| (%) increase in fbp | - | 24.64 | 22.45 | 20.98 |

The plot shown in Figure 4.13 clearly show blends 3 and 8 having close fbp which are higher than fbp recorded for blend 9. Blends 3 and 8 also have higher and more stable fracture

propagations as compared to blend 9. Table 4.7 shows the values of the fbp more clearly. These results are perfectly consistent with results obtained using sandstone cores where blend 3 gave the best result followed closely by blend 8. The fbp of blend 9 is closer to those of blends 3 and 8 in the concrete core test than in sandstone core due to 100% impermeable pores of the concrete, rendering the leak off of fluid from the induced fractures to the surrounding formation, impossible. These tests however, confirm repeatability of the experiments carried out with the sandstone cores. Achieving a fbp increase of about 25% in 100% impermeable concrete cores is a good indication that the fracturing fluid blends will be applicable to shale wellbore strengthening with potential substantial cost savings. Figure 4.14 shows an induced vertical fracture in concrete core.



Figure 4.14: Induced vertical fracture in concrete core

4.5 Experimental observations showing the absolute sealing effect of fracturing fluid

A very important and interesting observation was made while conducting these experiments that showed the absolute sealing capability of the fracturing fluid blend. Normally when a core/rock is fractured with a drilling/fracturing fluid and the fracture is allowed time to heal, upon commencement of the re-opening pressure cycle, the initial fracture will be re-opened and fluid will flow through this fracture. This is because fluid will always flow through the path of least resistance and this is the reason why the re-opening pressure is always almost the same with the fracture propagation pressure. It is never as high as the original fracture breakdown pressure (fbp) of the formation. However, it was noticed in two of the experiments performed; that on commencing the re-opening pressure cycle after 10 min fracture healing, that the initial fracture was totally sealed causing the fluid to initiate another vertical fracture. This means that cutting through the rock was the path of least resistance for the fluid rather than simply re-opening the already created fracture. This phenomenon was noticed in both the sandstone core and concrete core testing. This was noticed in the sandstone core using blend 4 which is when NP1 is set at high concentration and graphite set at high concentration. The same phenomenon was also noticed in the concrete core using blend 8 which is when NP2 is set at high concentration and graphite is set at high concentration as well. Two vertical fractures were noticed on the cores with the pressure profile plot of original breakdown pressure and re-opening pressure supporting these physical observations. This clearly shows the absolute sealing capability of the tested fracturing fluid blends which is a very desirable characteristic for wellbore strengthening. Figure 4.15 shows a sandstone core with two vertically induced fractures using blend 4 fracturing fluid while Figure 4.16 shows the corresponding pressure profile with re-opening pressure as high as original breakdown pressure.



Figure 4.15: Two vertically induced fractures using blend 4 on sandstone core

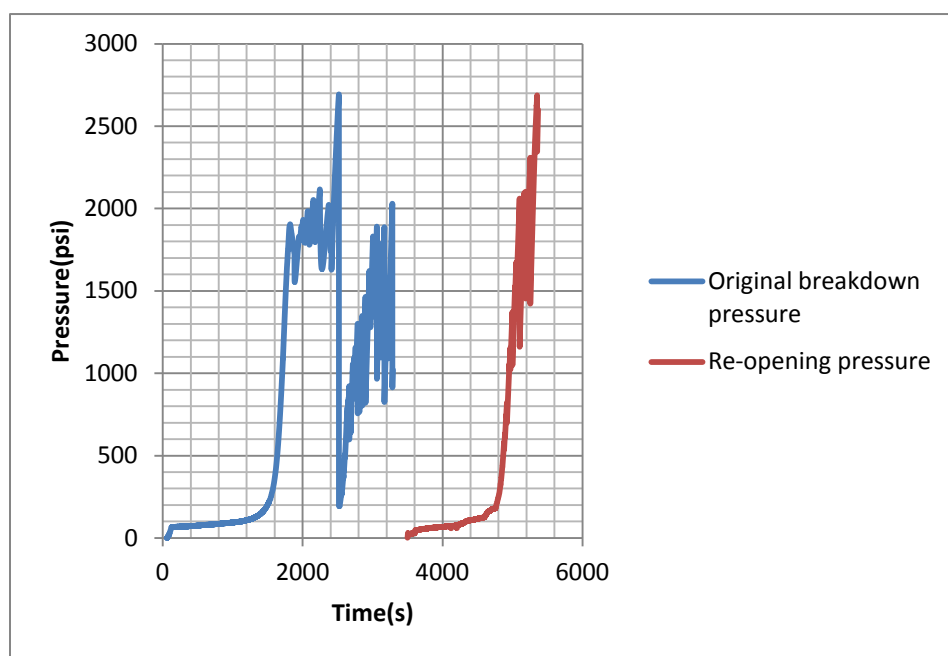


Figure 4.16: Showing re-opening pressure fbp as high as original fbp for the blend 4 test

Figure 4.17 shows two vertically induced fractures using blend 8 on the concrete core while Figure 4.18 shows the corresponding pressure profile with re-opening pressure as high as the original breakdown pressure.



Figure 4.17: Two vertically induced fractures using blend 8 on concrete core

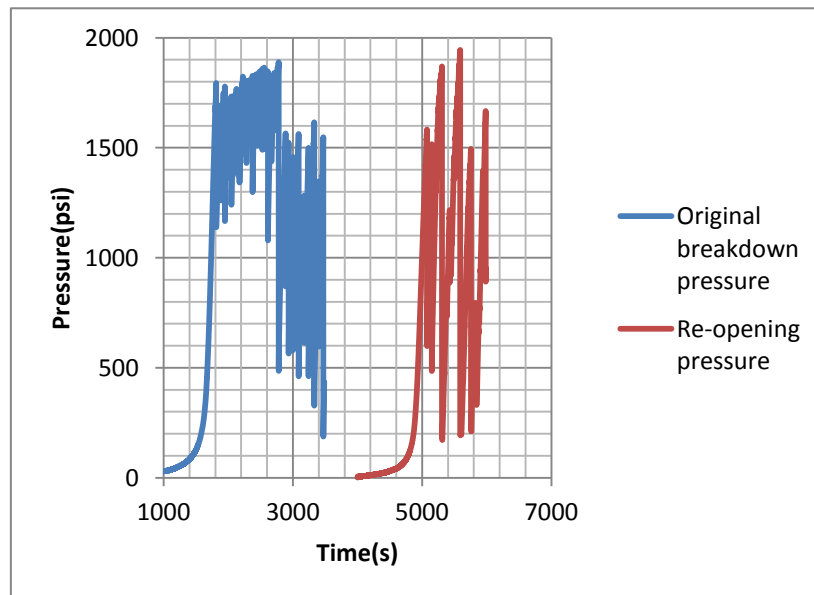


Figure 4.18: Showing re-opening pressure fbp as high as original fbp for the blend 8 test

4.6 Why Nano-particles (NPs) react better with WBM than with OBM

Both NPs used in this work have great affinity with organophilic clays due to the hydroxyl group (-OH) present on their surfaces which causes them to agglomerate in organic solution. NPs are held in the water by the addition of surfactants which prevents them from deagglomerating. Since the WBM is made up primarily of organophilic clays and water, it interacts strongly with the NPs thereby stabilizing the system. There is also electrostatic attraction between NPs and the rest of the fluid constituents with Van der Waals forces also helping to disperse the NPs well in the system. Due to the complex mixture of different constituents in OBM which prevent a strong bonding of the NPs to the system, the NPs are not as effective as in WBM.

4.7 Lessons learned

The following lessons were learned during the entire operation involved in carrying out the experiments for this work.

4.7.1 Core sample preparation operations

1. One of the main problems encountered while drilling out the cores from the slab was the issue of the cores being stuck in the coring bit after drilling through the rock slab. This problem was solved by turning the water jet supplying the core bit with cooling water to full blast. This ensured good hole cleaning efficiency, effectively removing the cuttings to the surface and preventing them from sticking the bit to the core.
2. Failure to adhere strictly to the surface grinding procedure will work against achieving a flat surface on the cores no matter how long one surface grinds. This is important because failure to achieve a totally flat surface will affect all other subsequent operations on the core and render the core unfit for the experiments.
3. The borehole position must be located in the center of the core. This is achieved by properly using the center finder to find the accurate center of the core.
4. Steel caps must be properly fixed on the core ensuring a perfect alignment with the core. This is very important because the pressure cell diameter is only marginally larger than the steel cap diameter and any shift of the core to any side of the cap will result in the core not fitting into the pressure cell after fixing the cap. This will result in the core getting stuck in the pressure cell and ultimately leading to loss of core and damage to pressure cell.

5. The core must be placed gently into the pressure cell to avoid shifting the O-ring out of place. Shifting the O-ring out of place will lead to loss of fluid from the core wellbore into the pressure cell preventing any pressure build up in the core.

4.7.2 Hydraulic fracture operations

1. The hydraulic fracture apparatus pipes and connectors are often clogged after each run of experiments due to the clogging nature of the fracturing fluid and the LCMs used. Thoroughly cleaning the pipes and connectors after conducting each experiment ensured this problem was avoided.
2. It was noted in the course of conducting these experiments that the experiments will run smoothly as planned only when injecting fluid into the core at 5ml/minute.
3. While injecting fluid into the core it was imperative to always check to confirm that the accumulator still had fracturing fluid left in it. This was carried out by monitoring the position of the piston rod sticking out of the accumulator. Failure to do this could lead to a damaged piston and erroneous readings.
4. It was noticed that occasionally both vertical and horizontal fractures were induced at the same time in the sandstone core. This is attributed to heterogeneity inherent in sedimentary rocks.

Chapter Five: **CONCLUSIONS**

The main objective of this work is to design an optimal nano-particles and granular particles lost circulation material (LCM) blend by running hydraulic fracture laboratory experiments and analyzing the results. In-house prepared nano-particles in combination with standard LCM-graphite have been used successfully in this project to achieve very impressive wellbore strengthening in sandstone and impermeable concrete cores. The following conclusions were reached after running all the experiments and analyzing the results from this work.

1. The optimal blend combination for water based mud (WBM) has been established. Optimal blend 3 (NP1-iron (III) hydroxide nano-particles set at low concentration) and granular particle A (graphite set at high concentration) increased fbp by 1,668.20 psi or by 70.31% over the fbp recorded with the WBM control sample.
2. The optimal blend combination for invert emulsion (diesel oil) based mud (OBM) has been established. Optimal blend 8 (NP2- calcium carbonate nano-particles set at high concentration) and granular particle A (graphite set at high concentration) increased the fbp by 586.8 psi or by 36.39% over the fbp recorded with the OBM control sample.
3. Plastic viscosity and 10 min gel strength are important markers or indicators that show when the fracturing fluid will give very good wellbore strengthening result.
4. There is a significant difference in the interaction of the nano-particles with the granular particles. The standard LCM-graphite gives a far better result in combination with the nano-particles, than calcium carbonate.
5. There is a significant difference in the fbp of the low density (8.8 lbs/gal) WBM and the low density (7.65 lbs/gal) OBM tested. The WBM fbp was 47.14% higher than that of the OBM.

6. Absolute fracture sealing was noticed in two of the experiments performed after running the re-opening pressure cycle. This clearly shows the excellent propping and sealing properties of the fracturing fluid.
7. The results observed using sandstone cores were validated using concrete cores thus confirming repeatability of experiments.
8. Wellbore strengthening was achieved in 100% impermeable concrete core with blend 3 fracturing fluid increasing fbp by 24.64% over the control sample recorded fbp.
9. The concrete core test result is a good indication that the fracturing fluid will give very good results when applied to wellbore strengthening in shale formations.
10. The optimal blends established at the end of this project have the potential of reducing drilling cost significantly by reducing the number of casings run while drilling through lost circulation zones.

Chapter Six: **RECOMMENDATIONS**

Based on the experimental work carried out and conclusions reached at the end of this work, the following recommendations for future work have been proposed.

1. Future work should utilize sandstones buried under the ground instead of the sandstones quarried from the outcrops. This will limit the heterogeneity experienced with the cores for a more objective assessment.
2. A stronger O-ring that can withstand pressures over 4,000 psi without failing should be used in the hydraulic fracture apparatus. This will ensure that the re-opening pressure cycle tests can be performed after 4,000 psi fbp has been achieved in the first injection pressure cycle.
3. Further tests combining graphite with other non-reactive LCMs like walnut, along with nano-particles, should be carried out using the established blends for WBM and OBM. This can further improve the results achieved in this work.
4. Adding fluid loss agents to the OBM optimal blend will further increase wellbore strengthening efficiency of the fluid.
5. Tests should be carried out using mineral oil based mud and synthetic oil based mud using the optimal blends to ascertain and compare the results with that of the already tested OBM.
6. Tests should be carried out on shale cores using the established optimum blends. This will confirm and ascertain the level of wellbore strengthening that can be achieved as suggested by the concrete cores.

7. Field tests should be carried out using the designed optimal blends for both WBM and OBM to investigate the effectiveness of the drilling fluid LCM blend in actual drilling conditions.

References

1. Kumar, A., Savari, S., Whitfill, D.L., and Jamison, D.E. "Wellbore strengthening: The less studied properties of lost circulation materials." *SPE ATCE*. Florence, Italy, 19-22 September 2010.
2. Drilling Specialities Company. "Lost Circulation Guide." Engineering CD, July 2006.
3. Dupriest, F. E. "Fracture Closure Stress (FCS) and Lost Returns Practices." *SPE/IADC Drilling Conference*. Amsterdam, Netherlands, 23-25 February 2005.
4. Salehi, S., and Nygaard, R. "Evaluation of New Drilling Approach for Widening Operational Window: Implications for wellbore strengthening." *SPE Production and Operations Symposium*. Oklahoma city, USA, 27-29 March 2011.
5. Morita, N., and Fuh, G.F. "Theory of Lost Circulation Pressure." *65th Annual SPE/ATCE*. New Orleans, LA., 23-26 September 1990.
6. Onyia, E.C. "Experimental Data Analysis of Lost-Circulation Problems During Drilling With Oil-Based Mud." *SPE Drilling & Completion*, March 1994.
7. Oort, E.V., Friedheim, J., Pierce, T., and Lee, J. "Avoiding Losses in Depleted and Weak Zones by Constantly Strengthening Wellbores." *SPE Drilling & Completion*, December 2011.
8. Alberty, M.W., and Mclean, M.R. "A physical model for stress cages." *SPE ATCE*. Houston, Texas, 26-29 September 2004.
9. Settari, A. "Reservoir Geomechanics-A Simulation Perspective." *Reservoir Geomechanics Lecture Notes*, Department of Chemical and Petroleum Engineering, University of Calgary. Calgary, Canada, 2011.
10. Amanullah, M., Al-Arfaj, M.K., and Al-Abdullatif, Z. "Preliminary test results of nano based drilling fluids for oil and gas application." *SPE/IADC Drilling Conference and Exhibition*. Amsterdam, Netherlands, 1-3 March 2011.
11. Amanullah, M., and Al-Tahini, A.M. "Nano-Technology-Its Significance in Smart Fluid Development for Oil and Gas Field Application." *SPE Saudia Arabia Section Technical Symposium and Exhibition*. Alkhobar, Saudi Arabia, 09-11 May 2009.
12. Sensoy, T., Chenevert, M.E., and Sharma, M.M. "Minimizing Water Invasion in Shale Using Nanoparticles." *SPE/ATCE*. New Orleans, Louisiana, USA, 4-7 October 2009.

13. Liberman, M. "Hydraulic Fracturing Experiments to Investigate Circulation Losses." M.Sc Petroleum Engineering Dissertation, Missouri University of Science and Technology. Rolla, Missouri, USA, 2012.
14. Traugott, D., Sweatman, R., and Vincent, R. "Increasing the Wellbore Pressure Containment in Gulf of Mexico HP/HT Wells." SPE Drilling & Completion, March 2007.
15. Dupriest, F.E., Smith, M.V., Zeilinger, C.S., and Shoykhet, I.N. "Method to Eliminate Lost Returns and Build Integrity Continuously With High-Filtration-Rate Fluid." SPE/IADC Drilling Conference. Orlando, Florida, USA, 4-6 March 2008.
16. Fuh, G.F., Beardmore, D., and Morita, N. "Further Development, Field Testing, and Application of the Wellbore Strengthening Technique for Drilling Operations." SPE/IADC Drilling Conference. Amsterdam, Netherlands, 20-22 February 2007.
17. Fuh, G.F., Morita, N., Boyd, P.A., and McGoffin, S.J. "A new Approach to Preventing Lost Circulation While Drilling." SPE ATCE. Washington , DC, USA, 4-7 October 1992.
18. Wang, H., Soliman, M.Y., and Towler, B. F. "Investigation of Factors for Strengthening a Wellbore by Propping Fractures." SPE Drilling & Completion, September 2009.
19. Song, J.H., and Rojas, J.C. "Preventing Mud Losses by wellbore strengthening." Russian oil and gas technical conference and exhibition. Moscow, 3-6 October 2006.
20. Aston, M.S., Alberty, M.W., Mclean, M.R., de Jong, H.J., and Armagost, K. "Drilling Fluids for wellbore strengthening." SPE/IADC Drilling Conference . Dallas, Texas, 2-4 March 2004.
21. Barrett, S., Cassanelli, J.P., Manescu, G., Vasquez, G., and Growcock, F. "Wellbore Strengthening-Where Field Application Meets Theory." SPE Latin American & Caribbean Petroleum Engineering Conference. Lima, Peru, 1-3 December 2010.
22. Wang, H., Soliman, M.Y., Towler, B.F., and Shan, Z. "Strengthening a wellbore with multiple fractures: further investigation of factors for strengthening a wellbore." ARMA conference. Asheville, June 28-July 1, 2009.
23. Wang, H., Soliman, M.Y., Towler, B.F., and Mukai, D. "Avoiding Drilling Problems by Strengthening the Wellbore While Drilling." 42nd US Rock Mechanics Symposium and 2nd U.S.-Canada Rock Mechanics Symposium. San Francisco, 29 June-2 July 2008.
24. Heinemann, Z.E. "Fluid Flow in Porous Media." Textbook Series, Volume 1, Montanuniversitat Leoben, 2005.

APPENDIX A: PRESSURE CELL ASSEMBLY AND EXPERIMENTAL SET UP

CHECK LIST

| | |
|---|--------------------------|
| 1. Raise Pressure Cell | <input type="checkbox"/> |
| 2. Remove Cutter Pins located on the back side of the Clevis Pins | <input type="checkbox"/> |
| 3. Remove Clevis Pins | <input type="checkbox"/> |
| 4. Lower Pressure Cell | <input type="checkbox"/> |
| 5. Place Teflon tape onto the injection nipple threads | <input type="checkbox"/> |
| 6. Place Teflon tape onto the injection pipe threads | <input type="checkbox"/> |
| 7. Screw injection pipe onto the injection nipple | <input type="checkbox"/> |
| 8. Place o-ring on the bottom of the core holder (inside Pressure Cell) | <input type="checkbox"/> |
| 9. Place the sample carefully inside the Pressure Cell | <input type="checkbox"/> |
| 10. Screw the injection line onto the sample | <input type="checkbox"/> |
| 11. Place Top Spacer 1 onto the sample | <input type="checkbox"/> |
| 12. Place o-ring onto the Top Spacer 1 | <input type="checkbox"/> |
| 13. Place Top Spacer 2 onto the Top Spacer 1 | <input type="checkbox"/> |
| 14. Place o-ring onto the Top Spacer 2 | <input type="checkbox"/> |
| 15. Place Top cap onto the Top spacer 2 | <input type="checkbox"/> |
| 16. Raise the Pressure Cell to desired height | <input type="checkbox"/> |
| 17. Place Clevis Pins | <input type="checkbox"/> |
| 18. Drop Pressure Cell onto the Clevis Pins until the hoist cables are no longer in tension | <input type="checkbox"/> |

| | |
|--|--|
| 19. Place Cutter Pins located on the back side of the Clevis Pins | |
| 20. Screw injection line from the Pressure Cell onto the injection line on the Wall | |
| 21. Screw confining line on the wall onto the Pressure Cell confining nipple | |
| 22. Screw air flush line from the Pressure Cell onto the air flush line on the Wall | |
| 23. Close confining exit valve | |
| 24. Open confining intake valve | |
| 25. Close air supply valve located on the vacuum pump | |
| 26. Close the valve on the overburden pump | |
| 27. Apply overburden until desired pressure | |
| 28. Fill up confining until desired pressure | |
| 29. Empty mud accumulator | |
| 30. Refill mud accumulator with desired mud | |
| 31. Remove air from the accumulator | |
| 32. Open Isco pump software | |
| 33. Assign a name to project click on check mark else your file will be saved under DATA.csv | |
| 34. Connect the pump to the computer | |
| 35. Check that pumps are filled before starting to inject into the accumulator | |
| 36. Open mud exit valve on the bottom of the Pressure Cell | |

| | |
|---|--------------------------|
| 37. Inject mud until little to no air comes out of the mud exit valve line | <input type="checkbox"/> |
| 38. Close mud exit valve | <input type="checkbox"/> |
| 39. Start recording data | <input type="checkbox"/> |
| 40. Start first injection cycle until there is a change in the Confining gauge | <input type="checkbox"/> |
| 41. Stop pumping after the first breakdown has been achieved | <input type="checkbox"/> |
| 42. Start timing for how long you are going to wait until your next cycle | <input type="checkbox"/> |
| 43. Open the mud exit valve | <input type="checkbox"/> |
| 44. Close the mud exit valve | <input type="checkbox"/> |
| 45. Check if the pumps must be refilled | <input type="checkbox"/> |
| 46. Start pumping the second cycle until there is a change in the Confining gauge | <input type="checkbox"/> |
| 47. Once all cycles are finished stop recording | <input type="checkbox"/> |
| 48. Put the pumps on Local control | <input type="checkbox"/> |
| 49. Remove Overburden Pressure | <input type="checkbox"/> |
| 50. Open Confining exit valve | <input type="checkbox"/> |
| 51. Close vacuum valve on the vacuum pump | <input type="checkbox"/> |
| 52. Open air intake valve on the vacuum pump | <input type="checkbox"/> |
| 53. Connect air flush hose onto the vacuum pump hose | <input type="checkbox"/> |
| 54. Open the system air flush valve located on the T connection on the vacuum pump | <input type="checkbox"/> |
| 55. Once air comes out of the Confining exit line close all valves at the vacuum pump | <input type="checkbox"/> |

| | |
|---|--|
| 56. Remove the air supply hose | |
| 57. Close the Confining exit valve | |
| 58. Unscrew injection line from the Pressure Cell onto the injection line on the Wall | |
| 59. Unscrew confining line on the wall onto the Pressure Cell confining nipple | |
| 60. Unscrew air flush line from the Pressure Cell onto the air flush line on the Wall | |
| 61. Raise the Pressure Cell | |
| 62. Remove Cutter Pins | |
| 63. Remove Clevis Pins | |
| 64. Lower the Pressure Cell until desired height | |
| 65. Remove Top Cap | |
| 66. Remove Top Spacer 2 | |
| 67. Remove Top Spacer 1 | |
| 68. Unscrew the injection line onto the sample | |
| 69. Pull sample out of cell from injection pipe | |
| 70. Carefully remove the sample | |
| 71. Remove o-ring from bottom of the core holder | |
| 72. Clean all residue of mud inside the core chamber | |
| 73. Raise the Pressure Cell | |
| 74. Place Clevis Pins | |

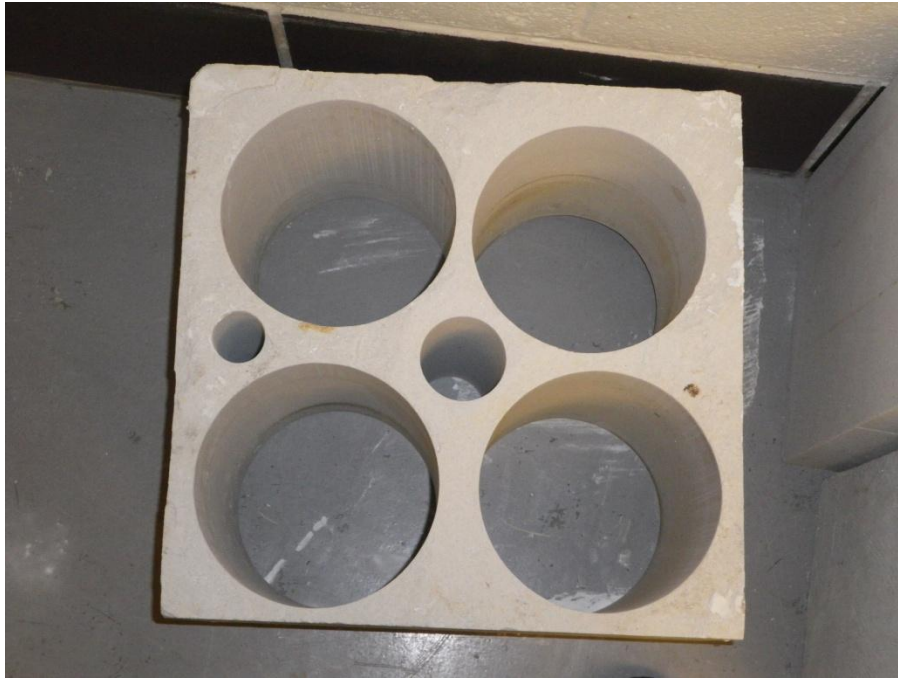
| | |
|---|--|
| 75. Drop Pressure Cell onto the Clevis Pins until the hoist cables are no longer in tension | |
|---|--|

| | |
|-----------------------|--|
| 76. Place Cutter Pins | |
|-----------------------|--|

APPENDIX B: CORE PREPARATION PICTURES



Drill press set up for coring rectangular sandstone slab



Rectangular slab after coring operation



Cylindrical cores drilled out from rectangular sandstone slab



Cutting off the rough edges of the cylindrical core with a slab saw



Surface grinding cylindrical core with surface grinder



Drill press set up for drilling borehole in the center of the core



Cylindrical cores with boreholes in the center



Cementing and clamping steel cap to core



Core with cemented caps on both sides before testing

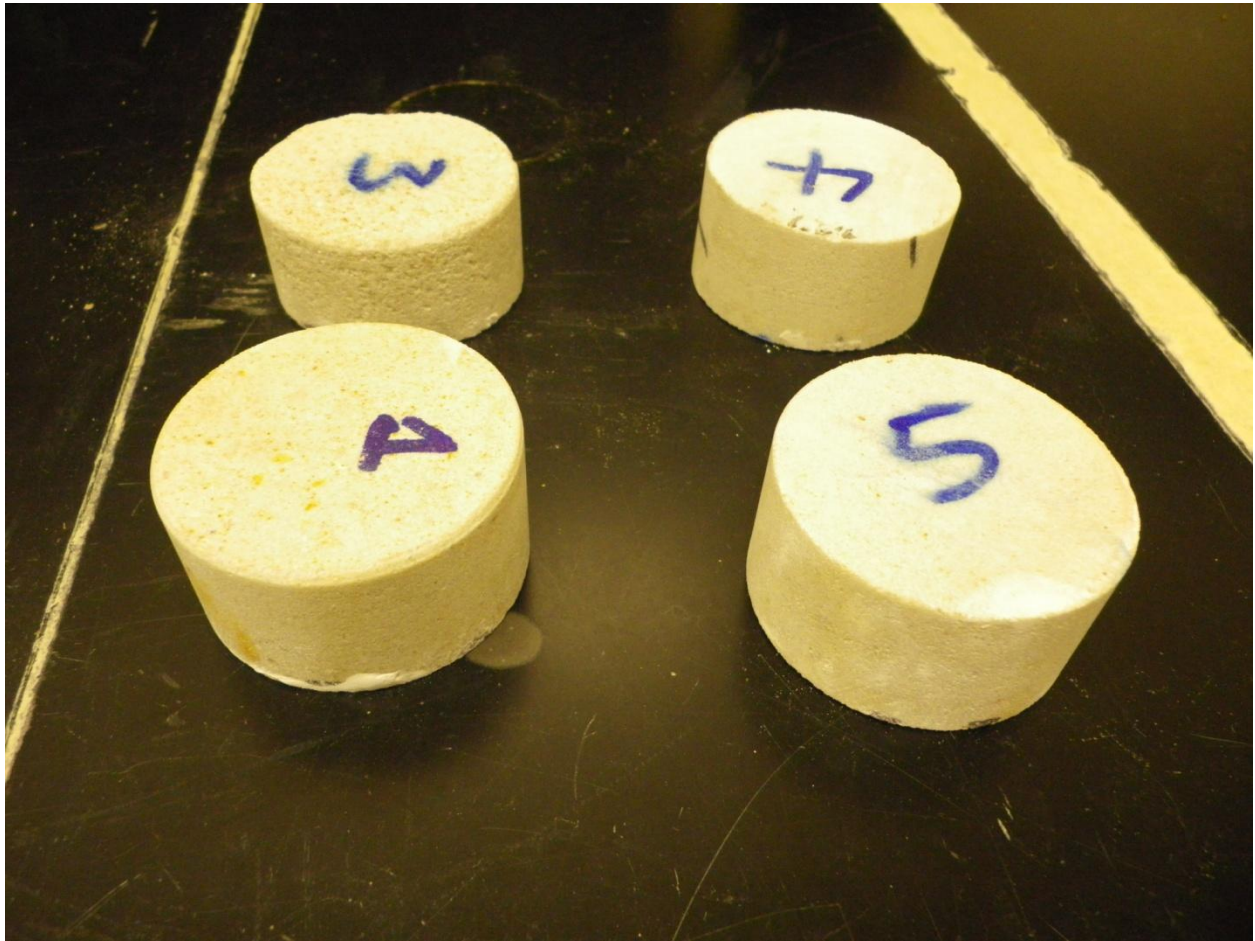


Core vacuuming apparatus set up

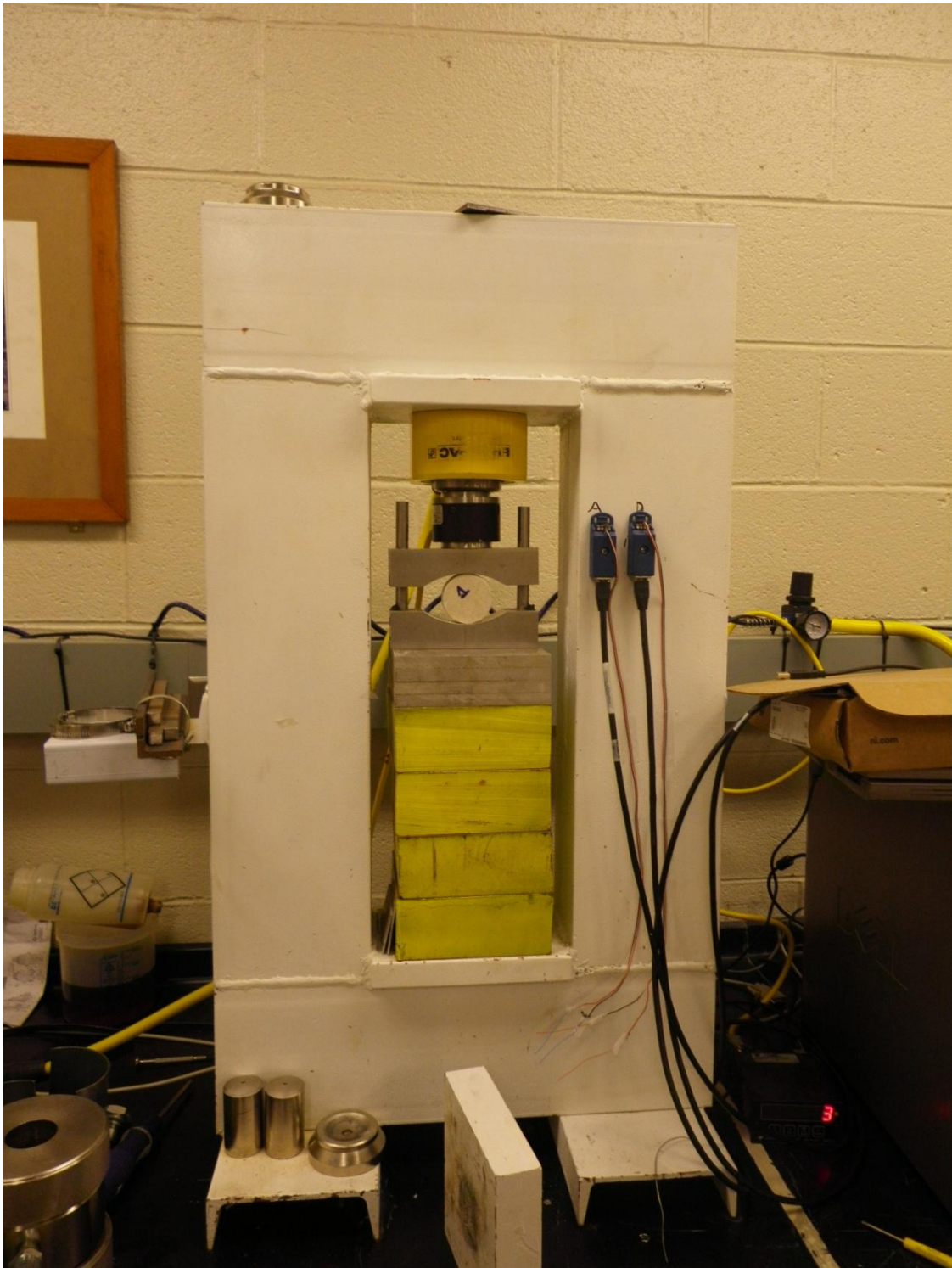


Cementing mix poured into metal core holders and left to cure

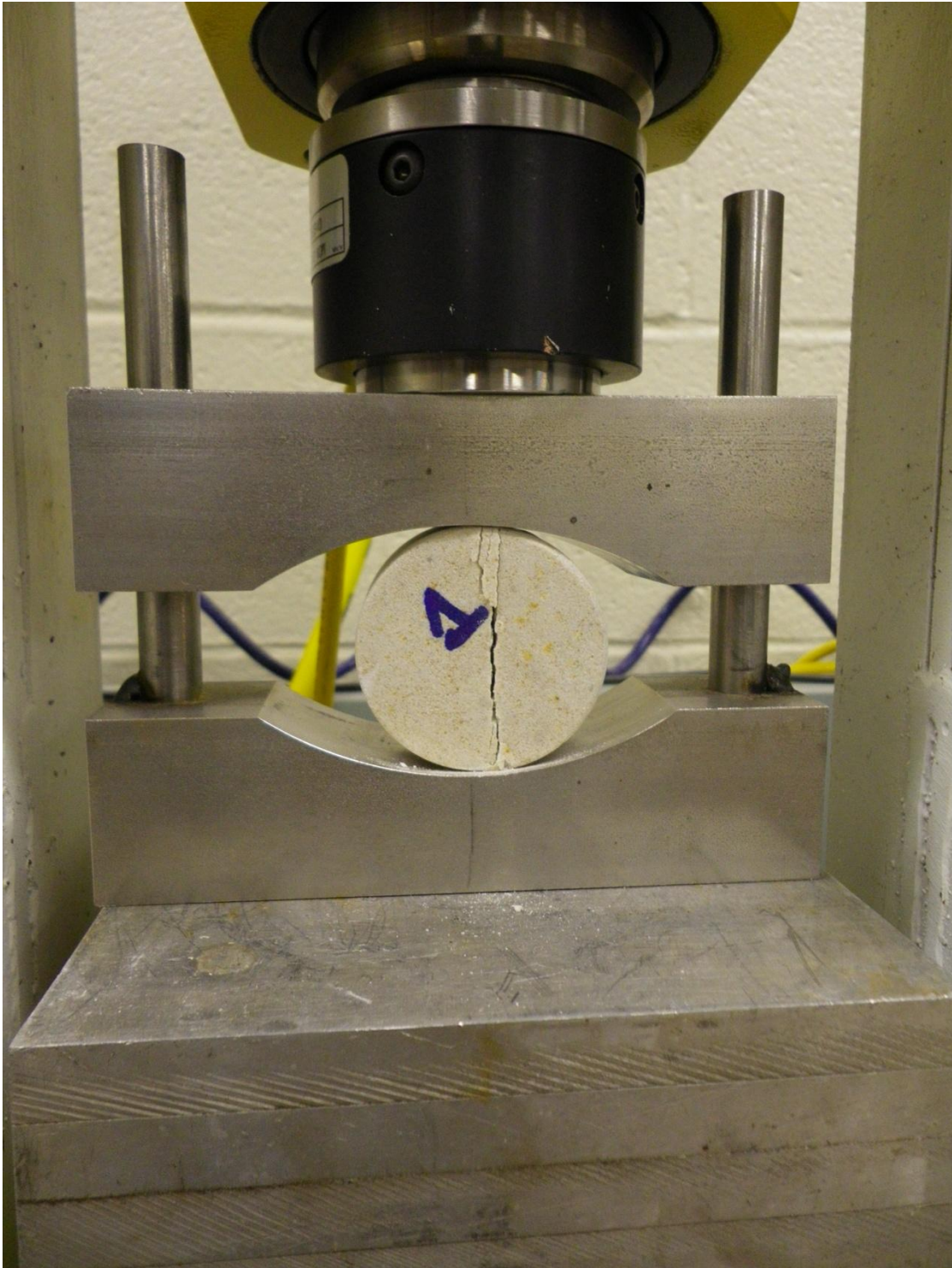
APPENDIX C: ROCK TENSILE STRENGTH MEASUREMENT PICTURES



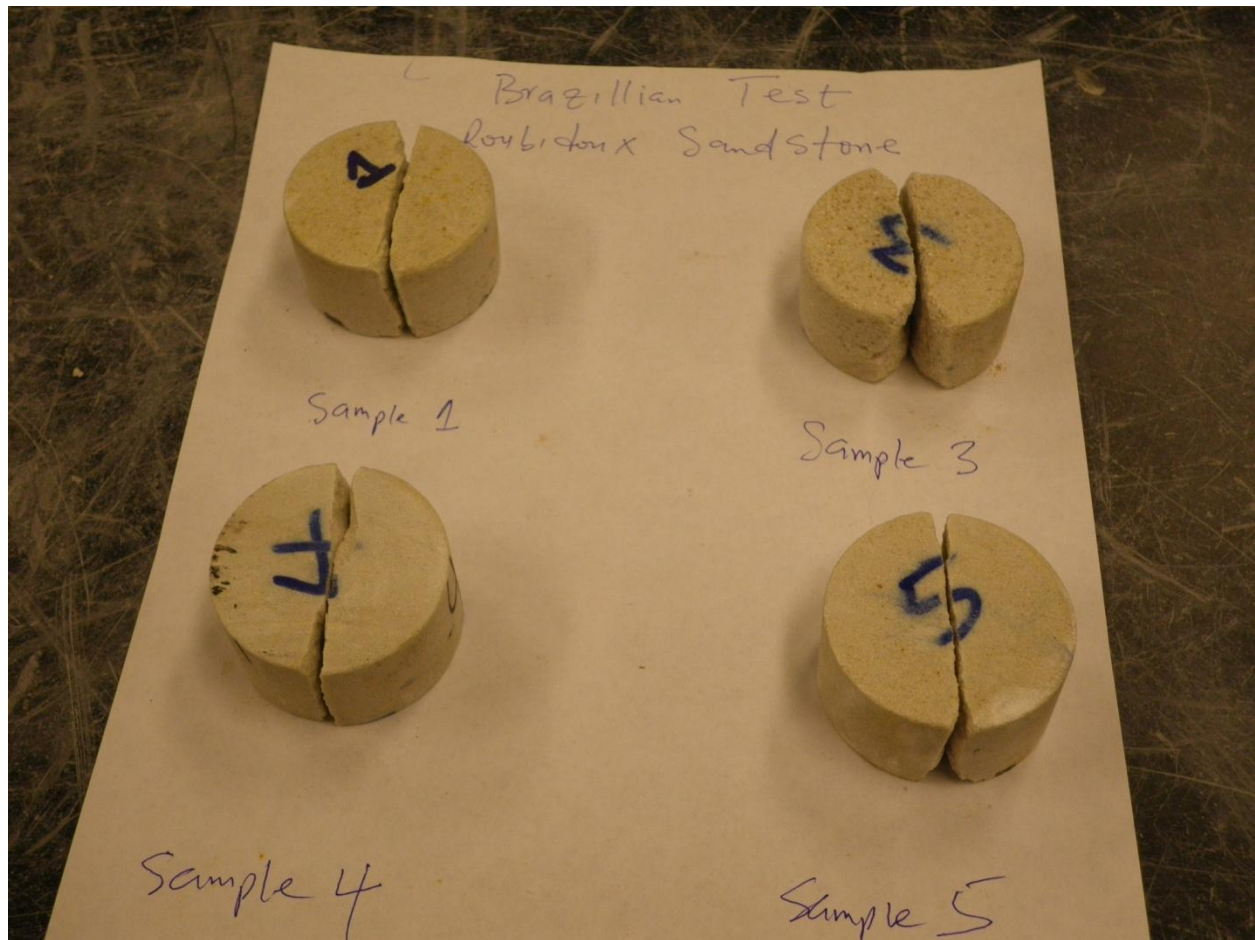
Core test samples before testing



Rock tensile strength measurement experimental set up



Core test sample at the point of failure



Core test samples after testing